European Journal of Taxonomy 452: 1–36
https://doi.org/10.5852/ejt.2018.452

ISSN 2118-9773
www.europeanjournaloftaxonomy.eu
2018 · Stec D. *et al.*



**Research article**

urn:lsid:zoobank.org:pub:76171A51-C284-455F-9504-C4CCEFE42D9D

# Integrative description of *Macrobiotus canaricus* sp. nov. with notes on *M. recens* (Eutardigrada: Macrobiotidae)

Daniel STEC [1,*], Łukasz KRZYWAŃSKI [2] & Łukasz MICHALCZYK [3]

[1,2,3] Department of Entomology, Institute of Zoology and Biomedical Research, Jagiellonian University, Gronostajowa 9, 30-387 Kraków, Poland.

[*] Corresponding author: daniel_stec@interia.eu
[2] Email: lukasz.s.krzywanski@gmail.com
[3] Email: LM@tardigrada.net

[1] urn:lsid:zoobank.org:author:C148C15D-9F12-4312-9702-B1E1513C63CC
[2] urn:lsid:zoobank.org:author:0B32C511-BC10-4946-8191-7623AF798C65
[3] urn:lsid:zoobank.org:author:6592787E-AAB1-4717-90C9-B967488F06F4

**Abstract.** In this paper we describe *Macrobiotus canaricus* sp. nov., a new tardigrade species of the *Macrobiotus hufelandi* group from the Canary Islands. Moreover, with the use of DNA sequencing, we confirm that *Macrobiotus recens* Cuénot, 1932 represents the *hufelandi* group, even though eggs laid by this species do not exhibit the typical *hufelandi* group morphology. Our study is based on both classical taxonomic methods that include morphological and morphometric analyses conducted with the use of light and scanning electron microscopy, and on the analysis of nucleotide sequences of four molecular markers (three nuclear: 18S rRNA, 28S rRNA, ITS-2, and one mitochondrial: COI). Our analyses revealed that *M. canaricus* sp. nov. is most similar to *Macrobiotus almadai* Fontoura *et al.*, 2008 from the Archipelago of the Azores, from which it differs by the absence of granulation patches on the external and internal surfaces of legs I–III as well as by the absence of a cuticular pore in the centre of the external patch on legs I–III. Molecular sequences allowed us to pinpoint the phylogenetic positions of *M. canaricus* sp. nov. and *M. recens* within the *M. hufelandi* group.

**Keywords.** Canary Islands, COI, *Macrobiotus hufelandi* group, phylogeny, tardigrades.

Stec D., Krzywański Ł. & Michalczyk Ł. 2018. Integrative description of *Macrobiotus canaricus* sp. nov. with notes on *M. recens* (Eutardigrada: Macrobiotidae). *European Journal of Taxonomy* 452: 1–36.
https://doi.org/10.5852/ejt.2018.452

## Introduction

Tardigrades are a phylum of globally distributed microinvertebrates which inhabit terrestrial and marine habitats (Nelson *et al.* 2015). However, the majority of the over 1200 known species were found and described from terrestrial mosses and lichens (Guidetti & Bertolani 2005; Degma & Guidetti 2007; Degma *et al.* 2009–2017). Although tardigrade faunistic studies have been conducted for more than two centuries, many regions are still very poorly known in terms of tardigrade species composition. One such place is the Canary Islands (Spain), where only two studies on tardigrades

have been performed until now (Heinis 1908; Guil & Guidetti 2005). In total, 13 taxa identified to species level have been reported from the Canary Islands: *Echiniscus arctomys* Ehrenberg, 1853, *E. canadensis* Murray, 1910, *E. quadrispinosus* Richters, 1902, *E. mediantus* Marcus, 1930, *E. trisetosus* Cuénot, 1932, *Isohypsibius tuberculatus* (Plate, 1888), *Macrobiotus echinogenitus* Richters, 1904, *M. furcatus* Ehrenberg, 1859, *M. hufelandi* C.A.S. Schultze, 1834, *M. occidentalis* Murray, 1910, *Milnesium tardigradum* Doyère, 1840, *Minibiotus intermedius* (Plate, 1888) and *M. gumersindoi* Guil & Guidetti, 2005. Moreover, both studies reported undetermined species of the *Macrobiotus hufelandi* group and Heinis (1908) noted an undetermined species of *Echiniscus* C.A.S. Schultze, 1840. However, not all of the thirteen species identifications can be considered certain according to modern taxonomic standards. For example, records of *M. hufelandi* and *M. tardigradum* predate the redescriptions of these species (Bertolani & Rebecchi 1993 and Michalczyk *et al.* 2012, respectively), and thus they need to be verified against modern literature.

We examined moss and lichen samples from the island of Gran Canaria. In two of them, we found two species of the *Macrobiotus hufelandi* group, one new to science and the other conforming to the description of *Macrobiotus recens* Cuénot, 1932. For both these populations, we provide taxonomic descriptions based on morphological and morphometric data acquired with phase contrast light microscopy (PCM) as well as from scanning electron microscopy (SEM). Additionally, we sequenced four DNA markers, three nuclear (18S rRNA, 28S rRNA, ITS-2) and one mitochondrial (COI), that allowed us to pinpoint the phylogenetic positions of the two species. Specimens of *M.* cf. *recens* conform to the diagnosis of the *hufelandi* group, but they lay eggs that depart from the typical *hufelandi* group egg ornamentation, i.e., instead of inverted goblet-shaped processes, the eggs are equipped with conical processes. Thus, the species either has not (Biserov 1990a, 1990b) or has (Bertolani & Rebecchi 1993; Kaczmarek & Michalczyk 2017b) been classified within the *hufelandi* group. Therefore, the first DNA sequences for *M. recens* allowed us to verify whether the species represents the *hufelandi* group.

## Material and methods

### Sample processing and tardigrade culturing

The moss and lichen samples containing the new species and *M.* cf. *recens*, respectively, were collected from two localities in Gran Canaria by Marta Kapała on 16 February 2017 (see Table 1 for details). Samples were examined for terrestrial tardigrades using standard methods described by Dastych (1980) with modification by Stec *et al.* (2015). A total of 21 individuals of the new species and 29 individuals of *M*. cf. *recens* were extracted from the first and the second sample, respectively. Live animals were placed in a culture to obtain more individuals and eggs required for integrative analyses (see Table 1 for details). Animals were reared on plastic Petri dishes according to the protocol in Stec *et al.* (2015).

### Microscopy and imaging

Specimens for light microscopy were mounted on microscope slides in a small drop of Hoyer's medium and secured with a cover slip, following the protocol in Morek *et al.* (2016b). Slides were then dried for five to seven days at 60 °C. Dried slides were sealed with a transparent nail polish and examined under a Nikon Eclipse 50i phase contrast light microscope (PCM) associated with a Nikon Digital Sight DS-L2 digital camera. In order to obtain clean and extended specimens for SEM, tardigrades were processed according to the protocol in Stec *et al.* (2015). In short, specimens were first subjected to a 60 °C water bath for 30 min to obtain fully extended animals, followed by a water/ethanol and an ethanol/acetone series, and then $CO_2$ critical point drying and finally sputter coated with a thin layer of gold. Specimens were examined under high vacuum in a Versa 3D DualBeam Scanning Electron Microscope at the ATOMIN facility of the Jagiellonian University, Kraków, Poland. Both studied populations were also examined for the presence of males with aceto-orcein staining (Bertolani 1971) in accordance with Stec *et al.* (2016a).

**Table 1.** Sample collection details and numbers of individuals and eggs used for integrative analyses of *M. canaricus* sp. nov. and *M.* cf. *recens* Cuénot, 1932. (PCM = phase contrast microscopy; SEM = scanning electron microscopy; DNA = DNA sequencing; ORC = orcein staining)

*****Eggs were taken from the culture and incubated individually until hatching, then the juveniles were used for DNA sequencing whereas egg chorions (isogenophores) were mounted on microscope slides in Hoyer's medium.

| Species | Sample code | Coordinates; altitude | Sample type, habitat | PCM | SEM | DNA | ORC |
|---|---|---|---|---|---|---|---|
| ***M. canaricus* sp. nov.** | ES.004 | 28°03′05″ N, 15°38′21″ W; 1050 m a.s.l. | moss on a tree trunk in a pine forest | 120 ind.<br>42 eggs | 20 ind.<br>15 eggs | 4 ind.<br>3 eggs* | 15 ind.<br>0 eggs |
| ***M.* cf. *recens*** | ES.006 | 28°02′38″ N, 15°40′22″ W; 885 m a.s.l. | lichen on a stone wall | 87 ind.<br>38 eggs | 8 ind.<br>10 eggs | 0 ind.<br>4 eggs* | 15 ind.<br>0 eggs |
| ***M. macrocalix*** | PL.110 | 49°31′27″ N, 21°02′23″ E; 254 m a.s.l. | moss on a roof | 60 ind.<br>72 eggs | 0 ind.<br>0 eggs | 4 ind.<br>0 eggs | 0 ind.<br>0 eggs |

All figures were assembled in Corel Photo-Paint X6, v. 16.4.1.1281. For structures that could not be satisfactorily focused in a single photograph, a stack of 2–8 images was taken with an equidistance of ca 0.2 μm and assembled manually into a single deep-focus image.

### Morphometrics and morphological nomenclature

All measurements are given in micrometres (μm). Sample size was adjusted following recommendations by Stec *et al.* (2016b). Structures were measured only if their orientation was suitable. Body length was measured from the anterior extremity to the end of the body, excluding the hind legs. The terminology used to describe oral cavity armature and egg shell morphology follows Michalczyk & Kaczmarek (2003) and Kaczmarek & Michalczyk (2017b). Macroplacoid length sequence is given according to Kaczmarek *et al.* (2014). Buccal tube length and the level of the stylet support insertion point were measured according to Pilato (1981). The *pt* index is the ratio of the length of a given structure to the length of the buccal tube expressed as a percentage (Pilato 1981). All other measurements and nomenclature are given in accordance with Kaczmarek & Michalczyk (2017b). In brief, the buccal tube width was measured as the external and internal diameter at the level of the stylet support insertion point. Lengths of the claw branches were measured from the base of the claw (i.e., excluding the lunula) to the top of the branch, including accessory points. Distance between egg processes was measured as the shortest line connecting base edges of the two closest processes. Morphometric data were handled using the 'Parachela' v. 1.3 template available from the Tardigrada Register (Michalczyk & Kaczmarek 2013). Tardigrade taxonomy follows Bertolani *et al.* (2014).

### Comparative material

The taxonomic key for the *hufelandi* group provided by Kaczmarek & Michalczyk (2017b) was used to determine whether the isolated species had previously been described. After one species could not be identified with the key, we compared it with the original description of the most similar species of the *hufelandi* group, *Macrobiotus almadai* Fontoura *et al.*, 2008. Additionally, we also compared our new species with three paratypes and one egg of *M. almadai* kindly loaned to us by Professor Paulo Fontoura. Moreover, thanks to the courtesy of Matteo Vecchi, we analysed photomicrographs of animals and eggs identified as '*M. recens*' by Maucci (1979) from several Portuguese populations deposited in the Maucci collection. Although our population conformed to the original description of *M. recens*, the description

**Table 2.** Primers and references for PCR protocols for amplification of the four DNA fragments sequenced in the study.

| DNA fragment | Primer name | Primer direction | Primer sequence (5'-3') | Primer source | PCR programme |
|---|---|---|---|---|---|
| **18S rRNA** | 18S_Tar_Ff1 | forward | AGGCGAAACCGCGAATGGCTC | Stec *et al.* (2017a) | Zeller (2010) |
| | 18S_Tar_Rr1 | reverse | GCCGCAGGCTCCACTCCTGG | | |
| **28S rRNA** | 28SF0001 | forward | ACCCVCYNAATTTAAGCATAT | Mironov *et al.* (2012) | Mironov *et al.* (2012) |
| | 28SR0990 | reverse | CCTTGGTCCGTGTTTCAAGAC | | |
| **ITS-2** | ITS2_Eutar_Ff | forward | CGTAACGTGAATTGCAGGAC | Stec *et al.* (2018c) | Stec *et al.* (2018c) |
| | ITS2_Eutar_Rr | reverse | TCCTCCGCTTATTGATATGC | | |
| **COI** | LCO1490 | forward | GGTCAACAAATCATAAAGATATTGG | Folmer *et al.* (1994) | Michalczyk *et al.* (2012) |
| | HCO2198 | reverse | TAAACTTCAGGGTGACCAAAAAATCA | | |

is outdated and, in our opinion, an accurate identification of the species is not possible until a modern redescription is available (see Discussion for more details). Therefore, we identified our population as *M.* cf. *recens*. Nevertheless, given that our population fits the description of *M. recens*, it has to represent at least a closely related species and, as such, it can be used to estimate the phylogenetic position of *M. recens* s.str.

### Genotyping

The DNA was extracted from individual animals following the Chelex® 100 resin (Bio-Rad) extraction method of Casquet *et al.* (2012) with modifications described in detail in Stec *et al.* (2015). We sequenced four DNA fragments, three nuclear (18S rRNA, 28S rRNA, ITS-2) and one mitochondrial (COI). All fragments were amplified and sequenced according to the protocols described in Stec *et al.* (2015); primers and original references for specific PCR programs are listed in Table 2. Sequencing products were read with the ABI 3130xl sequencer at the Molecular Ecology Lab, Institute of Environmental Sciences of the Jagiellonian University, Kraków, Poland. Sequences were processed in BioEdit v. 7.2.5 (Hall 1999) and submitted to GenBank.

### Comparative molecular analysis

For molecular comparisons, all published sequences of the four above-mentioned markers for species of the *hufelandi* complex were downloaded from GenBank (listed in Table 3). Additionally, we also sequenced the four DNA fragments for a new population of *Macrobiotus macrocalix* Bertolani & Rebecchi, 1993 collected in Łękawica, southern Poland by DS in October 2015 (see Table 1 for sample details). The sequences were aligned using the default settings (in the case of COI) and the Q-INS-I method (in the case of ribosomal markers: 18S rRNA, 28S rRNA and ITS-2) of MAFFT v. 7 (Katoh *et al.* 2002; Katoh & Toh 2008) and manually checked against non-conservative alignments in BioEdit. Then, the aligned sequences were trimmed to 763 (18S rRNA), 712 (28S rRNA), 317 (ITS-2) and 618 (COI), bp. All COI sequences were translated into protein sequences in MEGA7 v. 7.0 (Kumar *et al.* 2016) to check against pseudogenes. According to the recommendation by Srivathsan & Meier (2012), uncorrected pairwise distances were calculated using MEGA7 instead of genetic distances corrected by Kimura 2 parameter model (K2P).

### Data deposition

Raw morphometric measurements underlying the description of *Macrobiotus canaricus* sp. nov. are given in Supplementary Materials (SM.1) and are deposited in the Tardigrada Register (Michalczyk & Kaczmarek 2013) under www.tardigrada.net/register, whereas raw morphometric data underlying the description of the population of *M.* cf. *recens* are given in Supplementary Materials (SM.2). The DNA

**Table 3.** Sequences of species of the *Macrobiotus hufelandi* group used for molecular comparisons and the phylogenetic analyses of *Macrobiotus canaricus* sp. nov. and *M.* cf. *recens* Cuénot, 1932. Underlined GenBank accession numbers indicate type or neotype sequences, whereas bolded numbers indicate new sequences obtained in this study.

| DNA marker | Species | Accession number | Source |
|---|---|---|---|
| 18S rRNA | "*M. hufelandi*" Schultze, 1834 | GQ849024 | Giribet *et al.* (1996) |
| | *M. hufelandi* group species | HQ604971, FJ435738–40 | Bertolani *et al.* (2014), Guil & Giribet (2012) |
| | *M. hannae* Nowak & Stec, 2018 | MH063922 | Nowak & Stec (2018) |
| | "*M. joannae*" Pilato & Binda, 1983 [= *M. hannae* Nowak & Stec, 2018] | HQ604974–5 | Bertolani *et al.* (2014) |
| | *M. kristenseni* Guidetti *et al.*, 2013 | KC193577 | Guidetti *et al.* (2013) |
| | *M. macrocalix* Bertolani & Rebecchi, 1993 | HQ604976, **MH063926** | Bertolani *et al.* (2014), **this study** |
| | *M. papei* Stec *et al*., 2018 | MH063881 | Stec *et al*. (2018d) |
| | *M. paulinae* Stec *et al.*, 2015 | KT935502 | Stec *et al.* (2015) |
| | *M. polypiformis* Roszkowska *et al.*, 2017 | KX810008 | Roszkowska *et al.* (2017) |
| | *M. polonicus* Pilato *et al.*, 2003 | HM187580 | Wełnicz *et al.* (2011) |
| | *M. sapiens* Binda & Pilato, 1984 | DQ839601 | Bertolani *et al.* (2014) |
| | *M. scoticus* Stec *et al.*, 2017 | KY797265 | Stec *et al.* (2017b) |
| | *M. shonaicus* Stec *et al*., 2018 | MG757132 | Stec *et al*. (2018a) |
| 28S rRNA | *M. hannae* Nowak & Stec, 2018 | MH063924 | Nowak & Stec (2018) |
| | *M. hufelandi* group species | FJ435751, FJ435754–5 | Guil & Giribet (2012) |
| | *M. macrocalix* Bertolani & Rebecchi, 1993 | **MH063935** | **this study** |
| | *M. papei* Stec *et al*., 2018 | MH063880 | Stec *et al*. (2018d) |
| | *M. paulinae* Stec *et al.*, 2015 | KT935501 | Stec *et al.* (2015) |
| | *M. polypiformis* Roszkowska *et al.*, 2017 | KX810009 | Roszkowska *et al.* (2017) |
| | *M. scoticus* Stec *et al.*, 2017 | KY797266 | Stec *et al.* (2017b) |
| | *M. shonaicus* Stec *et al*., 2018 | MG757133 | Stec *et al*. (2018a) |
| ITS-2 | *M. hannae* Nowak & Stec, 2018 | MH063923 | Nowak & Stec (2018) |
| | *M. macrocalix* Bertolani & Rebecchi, 1993 | **MH063931** | **this study** |
| | *M. papei* Stec *et al*., 2018 | MH063921 | Stec *et al*. (2018d) |
| | *M. paulinae* Stec *et al.*, 2015 | KT935500 | Stec *et al.* (2015) |
| | *M. polonicus* Pilato *et al.*, 2003 | HM150647 | Wełnicz *et al.* (2011) |
| | *M. polypiformis* Roszkowska *et al.*, 2017 | KX810010 | Roszkowska *et al.* (2017) |
| | *M. sapiens* Binda & Pilato, 1984 | GQ403680 | Schill *et al.* (2010) |
| | *M. scoticus* Stec *et al.*, 2017 | KY797268 | Stec *et al.* (2017b) |
| | *M. shonaicus* Stec *et al*., 2018 | MG757134–5 | Stec *et al.* (2018a) |
| COI | *M. hannae* Nowak & Stec, 2018 | MH057764 | Nowak & Stec (2018) |
| | *M.*cf. *hufelandi*, Schultze, 1834 | HQ876589–94, HQ876596 | Bertolani *et al.* (2011a) |
| | *M. hufelandi*, Schultze, 1834 | HQ876584, HQ876586–8 | Bertolani *et al.* (2011a) |
| | *M. kristenseni* Guidetti *et al.*, 2013 | KC193575–6 | Guidetti *et al.* (2013) |
| | *M. macrocalix* Bertolani & Rebecchi, 1993 | FJ176203–07, FJ176208–17, HQ876571, **MH057767** | Cesari *et al.* (2009), Bertolani *et al.* (2011a) **this study** |
| | *M. papei* Stec *et al*., 2018 | MH057763 | Stec *et al*. (2018d) |
| | *M. paulinae* Stec *et al.*, 2015 | KT951668 | Stec *et al.* (2015) |
| | *M. polypiformis* Roszkowska *et al.*, 2017 | KX810011–2 | Roszkowska *et al.* (2017) |
| | *M. sandrae* Bertolani & Rebecchi, 1993 | HQ876566–67, HQ876569–70, HQ876562–73, HQ876574–83 | Bertolani *et al.* (2011a) |
| | *M. scoticus* Stec *et al.*, 2017 | KY797267 | Stec *et al.* (2017b) |
| | *M. shonaicus* Stec *et al*., 2018 | MG757136–7 | Stec *et al*. (2018a) |
| | *M. terminalis* Bertolani & Rebecchi, 1993 | JN673960, AY598775 | Cesari *et al.* (2011), Guidetti *et al.* (2005) |
| | *M. vladimiri* Bertolani *et al.*, 2011 | HM136931–2**,** HM136933–4, HQ876568 | Bertolani *et al.* (2011a, 2011b) |

sequences for the type population are deposited in GenBank (https://www.ncbi.nlm.nih.gov/genbank). Uncorrected pairwise distances are given in Supplementary Materials (SM.3).

**Phylogenetic analysis**

To verify the phylogenetic positions of the new species and *M.* cf. *recens*, phylogenetic trees were constructed using (1) all macrobiotid 18S rRNA sequences available from GenBank, (2) concatenated 18S rRNA+28S rRNA+ITS-2+COI sequences of macrobiotid species for which at least three of these markers were sequenced, and (3) all published *M. hufelandi* group COI sequences. In addition to the sequences of the *hufelandi* group listed in Table 3, we also used sequences of other species of the family Macrobiotidae published so far: Sands *et al.* (2008), Guidetti *et al.* (2009), Guil & Giribet (2012), Bertolani *et al.* (2014), Mapalo *et al.* (2016), Vecchi *et al.* (2016), Zawierucha *et al.* (2016), Mapalo *et al.* (2017), Stec & Kristensen (2017), Stec *et al.* (2018b). The sequences of *Milnesium variefidum* Morek *et al.*, 2016a and *Mi. berladnicorum* Ciobanu *et al.*, 2014 from Morek *et al.* (2016a) were used as the outgroup in the first two analyses, whereas four species of *Mesobiotus* served as the outgroup in the third analysis: *Me. ethiopicus* Stec & Kristensen, 2017, *Me. hilariae* Vecchi *et al.*, 2016, *Me. insanis* Mapalo *et al.*, 2017 and *Me. philippinicus* Mapalo *et al.*, 2016.

The sequences were aligned using the default settings (in the case of COI) and with the Q-INS-I method (in the case of ribosomal markers: 18S rRNA, 28S rRNA and ITS-2) of MAFFT v. 7 (Katoh *et al.* 2002; Katoh & Toh 2008) and then edited and checked manually in BioEdit. The alignments of 18S rRNA and COI sequences were trimmed to 739 bp and 618 bp, respectively, whereas the aligned sequences that were used to construct the concatenated data matrix were trimmed to: 728 bp (18S rRNA), 754 bp (28S rRNA), 570 bp (ITS-2) and 621 bp (COI). The sequences were concatenated in SequenceMatrix (Vaidya *et al.* 2011). The concatenated data matrix comprises species for which at least three of the aforementioned molecular markers are available. This resulted in only two gaps within the matrix: for the 18S rRNA sequence of *Me. insanis* (sequence too short) and the ITS-2 sequence of *Me. ethiopicus* (sequence not available). Using PartitionFinder v. 2.1.1 (Lanfear *et al.* 2016) under the Bayesian Information Criterion (BIC), the best scheme of partitioning and substitution models were chosen for posterior phylogenetic analysis. We ran the analysis to test all possible models implemented in the program. As the COI is a protein coding gene, before partitioning, we divided our alignments of this marker into 3 data blocks constituting separated three codon positions. As best-fit partitioning scheme, PartitionFinder always suggested the retention of all predefined partitions separately. See Table 4 for specific substitution models suggested for all tested data sets and partitions.

Bayesian inference (BI) marginal posterior probabilities were calculated for both data sets using MrBayes v. 3.2 (Ronquist & Huelsenbeck 2003). Random starting trees were used and the analysis was run for ten million generations, sampling the Markov chain every 1000 generations. An average standard deviation of split frequencies of $< 0.01$ was used as a guide to ensure the two independent analyses had converged. The program Tracer v. 1.7 (Rambaut *et al.* 2018) was then used to ensure Markov chains had reached stationarity and to determine the correct 'burn-in' for the analysis, which was the first 10% of generations. The ESS values were greater than 200 and a consensus tree was obtained after summarising the resulting topologies and discarding the 'burn-in'. All final consensus trees were viewed and visualised by FigTree v. 1.4.3, available from http://tree.bio.ed.ac.uk/software/figtree.

**Abbreviations**

PCM = phase contrast light microscopy
SEM = scanning electron microscopy
IZiBB = Institute of Zoology and Biomedical Research, Jagiellonian University, Kraków, Poland

**Table 4.** The best scheme of partitioning and substitution models chosen for posterior phylogenetic analysis using PartitionFinder v. 2.1.1 under the Bayesian Information Criterion (BIC). The analyses were run to test all possible models implemented in the program.

| Data set | Substitution model for the given partition | | | | | |
|---|---|---|---|---|---|---|
| | 18S | 28S | ITS-2 | COI-1st | COI-2nd | COI-3rd |
| **18S** | SYM+I+G | – | – | – | – | – |
| **COI** | – | – | – | SYM+I+G | GTR+I+G | TRN+G |
| **18S+28S+ ITS-2+COI** | SYM+G | GTR+G | SYM+G | GTR+I+G | GTR+I+G | GTR+G |

## Results

### Taxonomic account

Phylum Tardigrada Doyère, 1840
Class Eutardigrada Richters, 1926
Order Parachela Schuster *et al.,* 1980
Superfamily Macrobiotoidea Thulin, 1928 (in Marley *et al.* 2011)
Family Macrobiotidae Thulin, 1928
Genus *Macrobiotus* C.A.S. Schultze, 1834

***Macrobiotus canaricus*** sp. nov.
urn:lsid:zoobank.org:act:AE3AAEA9-D20E-4917-8ECD-12B30DB514B6
Figs 1–7, Tables 5–6

### Etymology

The specific epithet refers to the Canary Islands, the place where the new species was found.

**Material examined** (162 animals, 57 eggs)

Specimens mounted on microscope slides in Hoyer's medium (120 animals + 42 eggs), fixed on SEM stubs (20 + 15), processed for DNA sequencing (7 animals), and aceto-orcein staining (15 animals).

**Holotype**

SPAIN: Canary Islands, Gran Canaria, Fagajesto, 28°03′05″ N, 15°38′21″ W, moss on a tree trunk in a pine forest (slide IZiBB ES.004.04).

**Paratypes**

SPAIN: 127 specimens, same data as for holotype (slides IZiBB ES.004.01–24); 42 eggs, same data as for holotype (slides IZiBB ES.004.25–33).

### Description

**Animals** (measurements and statistics in Table 5)

Body white in adults, after fixation in Hoyer's medium transparent (Fig. 1A). Eyes present both in live animals and in specimens mounted in Hoyer's medium. Round and oval pores (0.4–0.7 μm in diameter), visible under PCM and SEM, scattered randomly on entire body cuticle (Fig. 2A–F), including external and internal surface of all legs (Fig. 2A–F). Extremely fine body granulation (granules 0.06–0.09 μm

**Table 5.** Measurements (in µm) of selected morphological structures of individuals of *Macrobiotus canaricus* sp. nov. mounted in Hoyer's medium (N = number of specimens / structures measured; Range = the smallest and the largest structure among all measured specimens; SD = standard deviation)

| Character | N | Range | | Mean | | SD | | Holotype | |
|---|---|---|---|---|---|---|---|---|---|
| | | µm | *pt* | µm | *pt* | µm | *pt* | µm | *pt* |
| Body length | 30 | 306–431 | *902–1206* | 368 | *1094* | 30 | *72* | 359 | *1088* |
| Buccopharyngeal tube | | | | | | | | | |
| Buccal tube length | 30 | 29.5–37.6 | – | 33.7 | – | 1.8 | – | 33.0 | – |
| Stylet support insertion point | 30 | 22.4–28.1 | *74.3–76.8* | 25.4 | *75.4* | 1.3 | *0.7* | 24.6 | *74.5* |
| Buccal tube external width | 30 | 3.2–5.4 | *10.3–15.5* | 4.3 | *12.8* | 0.4 | *1.1* | 4.3 | *13.0* |
| Buccal tube internal width | 30 | 2.1–3.3 | *6.6–9.5* | 2.7 | *7.9* | 0.3 | *0.8* | 2.5 | *7.6* |
| Ventral lamina length | 28 | 16.2–24.4 | *53.4–68.2* | 20.5 | *60.8* | 1.5 | *3.7* | 19.5 | *59.1* |
| Placoid lengths | | | | | | | | | |
| Macroplacoid 1 | 30 | 5.5–9.5 | *17.7–28.4* | 7.3 | *21.5* | 1.0 | *2.4* | 8.0 | *24.2* |
| Macroplacoid 2 | 30 | 4.6–7.1 | *14.6–20.5* | 5.8 | *17.2* | 0.6 | *1.4* | 6.0 | *18.2* |
| Microplacoid | 30 | 1.6–2.7 | *4.7–7.8* | 2.0 | *6.0* | 0.3 | *0.8* | 2.1 | *6.4* |
| Macroplacoid row | 30 | 11.5–17.5 | *36.8–52.0* | 14.1 | *41.8* | 1.4 | *3.1* | 14.4 | *43.6* |
| Placoid row | 30 | 14.0–19.4 | *42.6–55.3* | 16.6 | *49.2* | 1.5 | *3.0* | 17.0 | *51.5* |
| Claw 1 lengths | | | | | | | | | |
| External primary branch | 30 | 8.3–11.3 | *25.1–33.5* | 9.5 | *28.3* | 0.7 | *2.0* | 8.3 | *25.2* |
| External secondary branch | 30 | 6.2–9.3 | *19.0–26.2* | 7.4 | *22.1* | 0.7 | *1.9* | 6.5 | *19.7* |
| Internal primary branch | 29 | 7.5–10.6 | *23.8–32.0* | 9.2 | *27.4* | 0.6 | *1.9* | 8.6 | *26.1* |
| Internal secondary branch | 29 | 6.0–8.4 | *17.4–23.8* | 7.0 | *20.7* | 0.6 | *1.7* | 6.6 | *20.0* |
| Claw 2 lengths | | | | | | | | | |
| External primary branch | 30 | 8.6–11.8 | *25.3–35.6* | 9.8 | *29.3* | 0.7 | *2.2* | 9.0 | *27.3* |
| External secondary branch | 30 | 5.8–8.7 | *18.4–26.0* | 7.4 | *22.1* | 0.7 | *2.2* | 6.3 | *19.1* |
| Internal primary branch | 29 | 8.2–10.8 | *24.2–31.2* | 9.4 | *28.0* | 0.6 | *1.8* | 8.2 | *24.8* |
| Internal secondary branch | 29 | 5.4–8.6 | *15.9–25.1* | 7.2 | *21.5* | 0.6 | *2.0* | 7.4 | *22.4* |
| Claw 3 lengths | | | | | | | | | |
| External primary branch | 28 | 8.9–11.0 | *25.8–32.6* | 10.0 | *29.8* | 0.6 | *1.9* | 9.2 | *27.9* |
| External secondary branch | 28 | 6.4–9.7 | *18.8–28.4* | 7.7 | *22.8* | 0.7 | *2.4* | 7.2 | *21.8* |
| Internal primary branch | 28 | 5.6–11.3 | *16.5–31.6* | 9.5 | *28.1* | 1.0 | *3.0* | 8.1 | *24.5* |
| Internal secondary branch | 28 | 6.0–8.9 | *16.8–25.7* | 7.3 | *21.7* | 0.7 | *1.9* | 6.9 | *20.9* |
| Claw 4 lengths | | | | | | | | | |
| Anterior primary branch | 27 | 8.6–20.5 | *28.5–57.1* | 11.2 | *33.1* | 2.0 | *5.2* | 10.3 | *31.2* |
| Anterior secondary branch | 25 | 6.7–9.7 | *18.5–28.8* | 8.1 | *24.1* | 0.8 | *2.3* | 6.9 | *20.9* |
| Posterior primary branch | 26 | 9.6–13.2 | *28.3–37.6* | 11.2 | *33.2* | 0.8 | *2.7* | 10.5 | *31.8* |
| Posterior secondary branch | 23 | 6.6–9.5 | *19.4–27.3* | 8.1 | *24.0* | 0.9 | *2.3* | 7.4 | *22.4* |

in diameter), visible only under SEM, present on the dorso-posterior cuticle (Fig. 2E–F). Granulation patches on external surface of legs I–III clearly visible both under PCM and SEM (Fig. 3A–B). Granulation patches on internal surface of legs I–III weakly visible under PCM but clearly visible under SEM (Fig. 3C–D, empty indented arrowheads). Single, large, oval pore present at centre of each external patch on legs I–III (Fig. 3A–B, filled flat arrowheads). Cuticular bulge, resembling pulvinus, present on internal surface of legs I–III (Fig 3C–D, filled indented arrowheads). This structure is visible only if legs are fully extended and correctly oriented on slide. Cuticular granulation on legs IV present and always clearly visible both under PCM and SEM (Fig. 3E–F).

Mouth antero-ventral. Bucco-pharyngeal apparatus of the *Macrobiotus* type, with the ventral lamina and ten small peribuccal lamellae followed by six buccal sensory lobes (Fig. 4A–C). Under PCM, the oral cavity armature is of the *maculatus* type, i.e., only the third band of teeth is visible (Fig. 4A).

Under SEM, the oral cavity is always composed of three bands of teeth (Fig. 4B–C). The first band of teeth is composed of numerous extremely small cones arranged in one or two rows, situated anteriorly in the oral cavity, on the basal part of the peribuccal lamellae (Fig. 4B–C, filled arrowhead). The second band of teeth is situated between the ring fold and the third band of teeth and consists of cones, clearly larger than those of the first band (Fig. 4B–C, empty arrowhead). The teeth of the third band are located within the posterior portion of the oral cavity, between the second band of teeth and the buccal tube opening (Fig. 4B–C). The third band of teeth is discontinuous and divided into a dorsal and a ventral portion. Under PCM, the dorsal teeth form a transversal ridge weakly divided into three teeth, whereas the ventral teeth appear as two separate lateral transverse ridges between which a roundish median tooth is visible (Fig. 4A). Under SEM, the dorsal teeth are divided into three separate teeth: one median and two lateral, the median tooth has a slightly serrated edge (Fig. 4B). The ventral teeth are also separated into one median and two lateral teeth (Fig. 4C). The medio-ventral tooth is much smaller than the medio-dorsal tooth (Fig. 4B–C). Pharyngeal bulb spherical, with triangular apophyses, two rod-shaped macroplacoids and a small microplacoid (Fig. 4A). The first and the second macroplacoids have a fine central and a subterminal constriction, respectively. The macroplacoid length sequence is $2 < 1$.

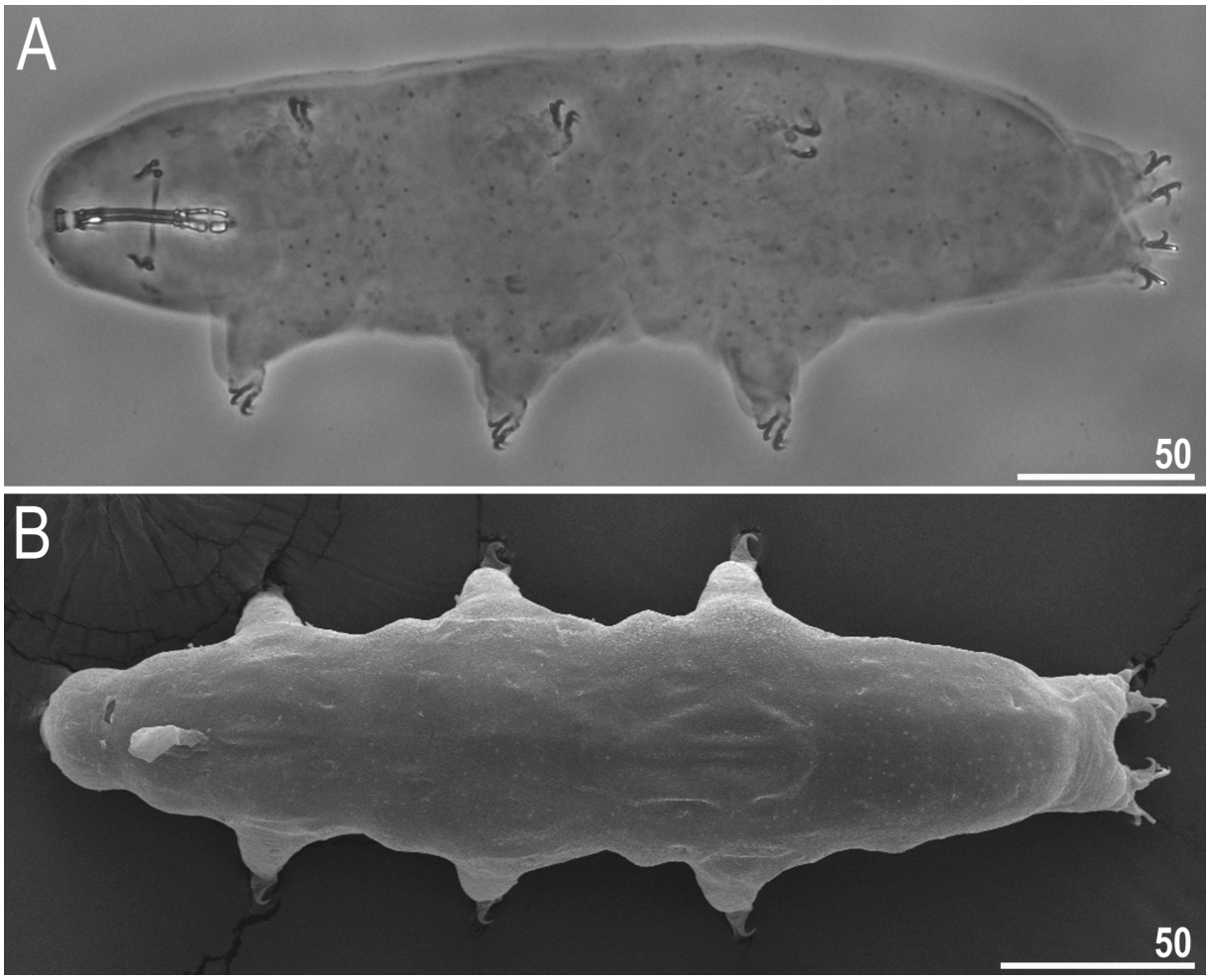


**Fig. 1.** *Macrobiotus canaricus* sp. nov., holotype, habitus. **A**. Dorso-ventral projection (Hoyer's medium, PCM). **B**. Dorsal view under SEM. Scale bars in μm.

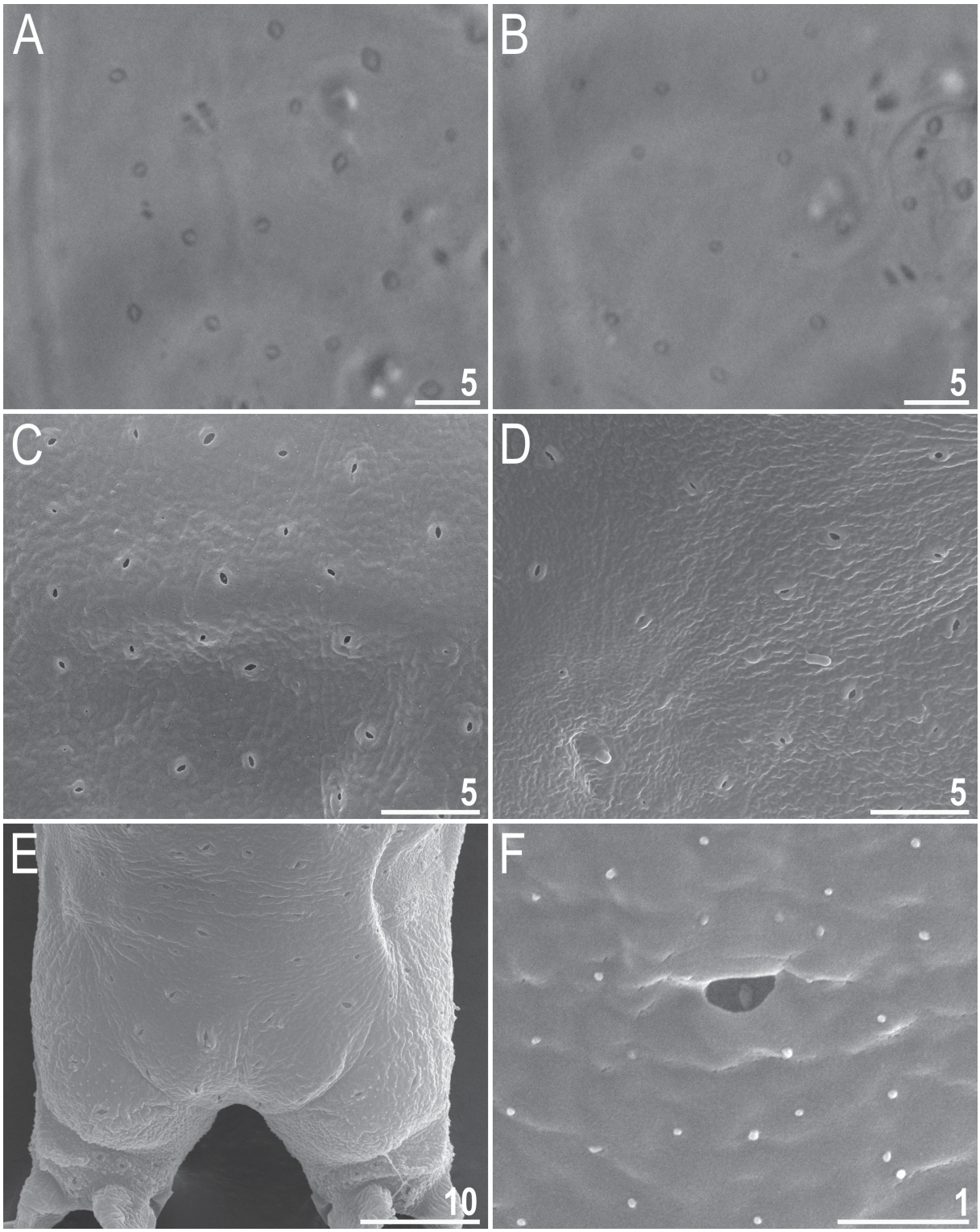


**Fig. 2.** *Macrobiotus canaricus* sp. nov., paratypes, body cuticle. **A–B**. Pores on the dorsal and ventral cuticle, respectively (PCM). **C–D**. Pores on the dorsal and ventral cuticle, respectively (SEM). **E**. Pores and fine granulation on the dorso-posterior cuticle (SEM). **F**. Close-up of a pore and granulation on the dorso-posterior cuticle (SEM). Scale bars in μm.

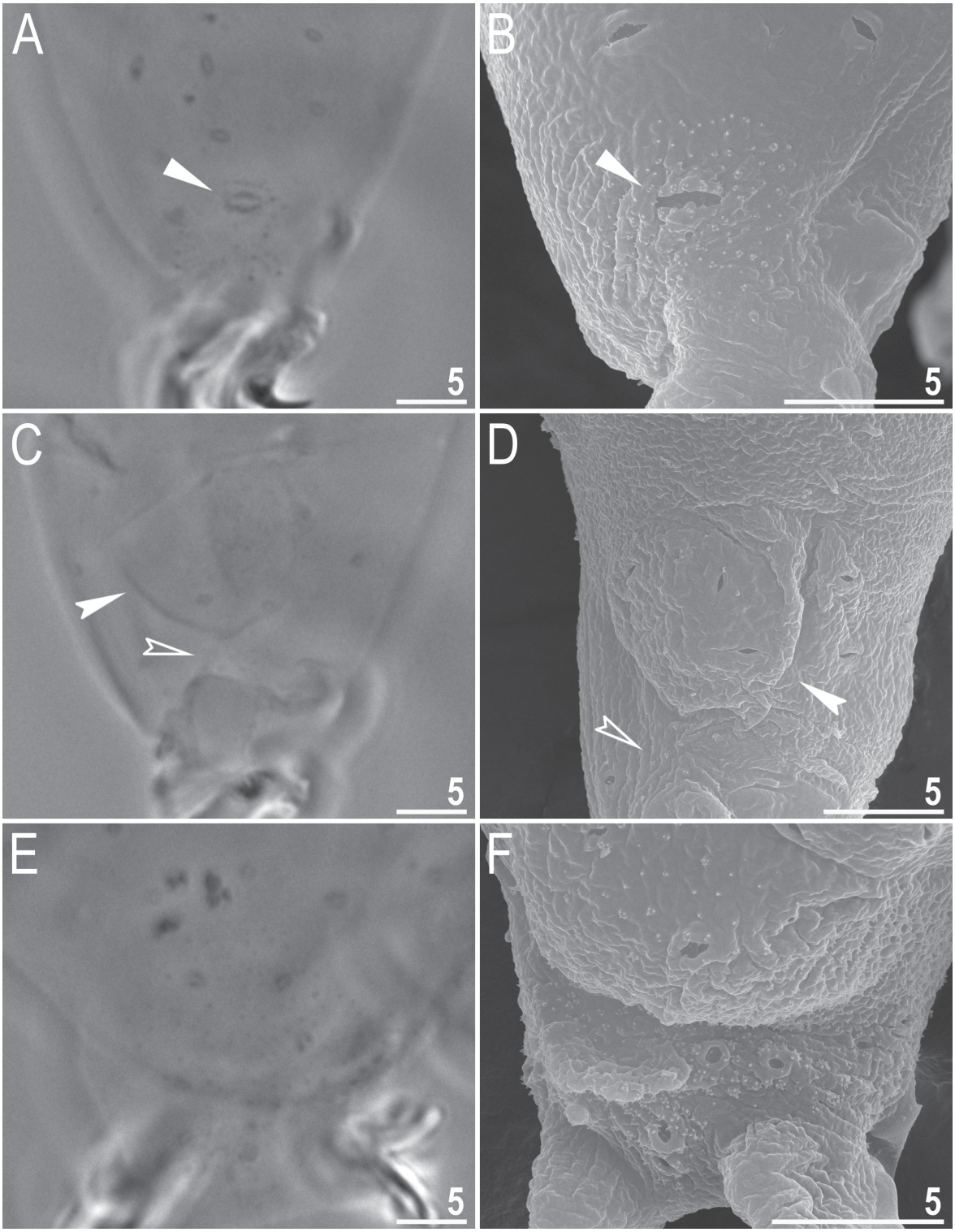


**Fig. 3.** *Macrobiotus canaricus* sp. nov., paratypes, cuticular structures on legs. **A–B**. The patch of granulation on the external surface of leg III with a large oval cuticular pore at the centre of the patch (PCM and SEM, respectively). **C–D**. The patch of granulation and the cuticular bulge (pulvinus) on the internal surface of leg II (PCM and SEM, respectively). **E–F**. Granulation on leg IV (PCM and SEM, respectively). Filled flat arrowheads indicate the large pore in the centre of the external granulation patch, filled indented arrowheads indicate the cuticular fold (pulvinus) on the internal leg surface, and empty indented arrowheads indicate granulation on the internal leg surface. Scale bars in μm.

Claws Y-shaped, of the *hufelandi* type (Fig. 5A–D). Primary branches with distinct accessory points and with an evident stalk connecting the claw to the lunula (Fig. 5A–D). Lunulae under all claws smooth (Fig. 5A–D). Cuticular bars under claws absent but muscle attachments are visible under claws I–III (Fig. 5A, C, filled arrowhead).

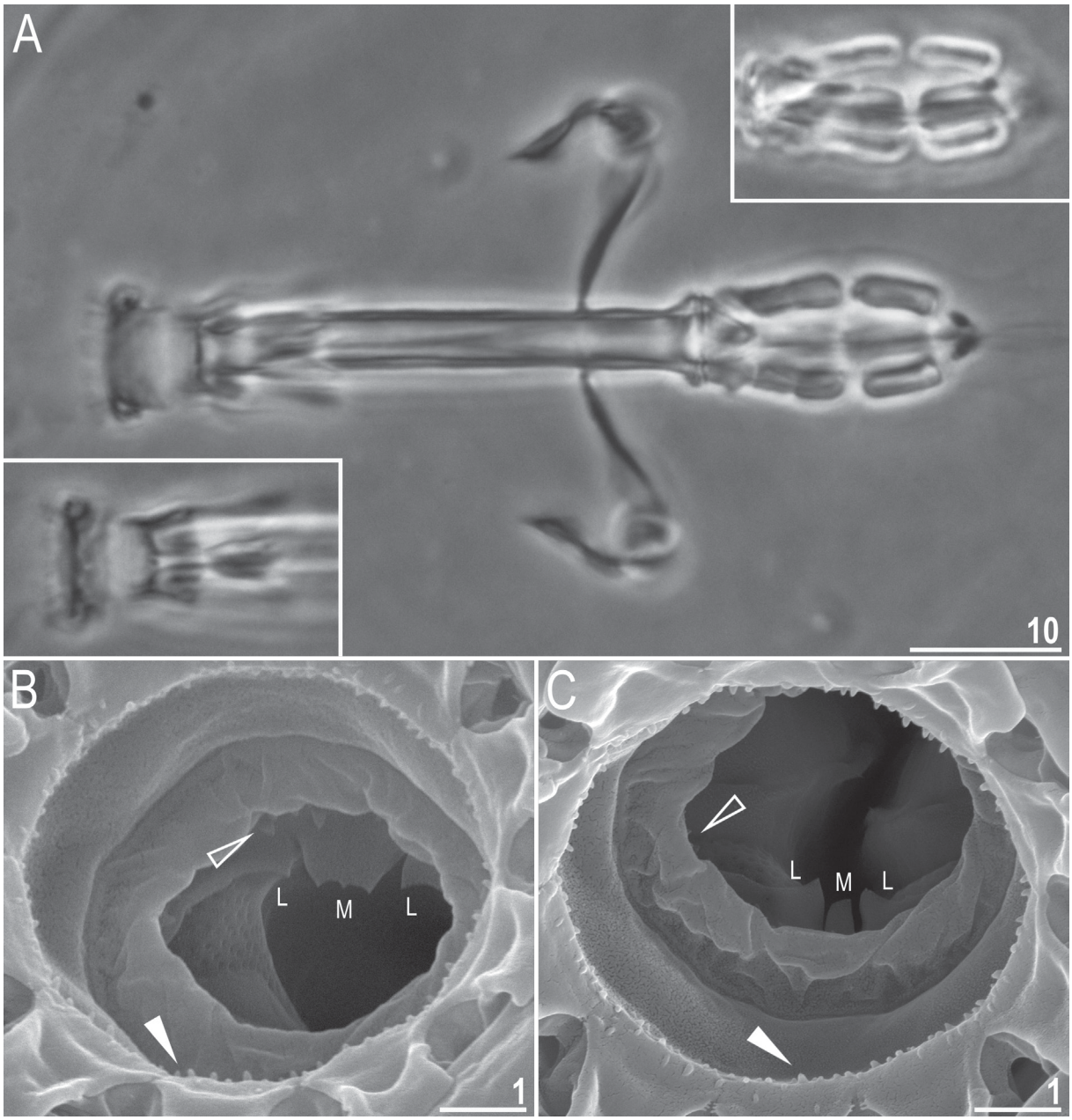


**Fig. 4.** *Macrobiotus canaricus* sp. nov., paratypes, buccal apparatus and the oral cavity armature seen under PCM and SEM. **A**. Dorsal projection of the entire buccal apparatus; the lower insert shows a ventral view of the oral cavity armature, the upper insert shows macroplacoid morphology (PCM). **B–C**. The oral cavity armature of a single paratype seen under SEM from different angles. Filled arrowheads indicate the teeth of the first band, empty arrowheads indicate the teeth of the second band, median teeth are marked with M, andlateral teeth are marked with L. Scale bars in μm.

**Eggs** (measurements and statistics in Table 6)

Laid freely, white, spherical or slightly oval (Figs 6A–B, 7A). The surface between processes of the *hufelandi* type, i.e., covered by a reticulum with very thin walls (Figs 6D–E, 7A–F). Peribasal meshes slightly larger and with slightly thicker walls compared to interbasal meshes (Figs 6D–E, 7B–F). The mesh diameter is always larger then mesh walls and nodes/knots (Figs 6D–E, 7B–F). The meshes are 0.3–1.0 μm in diameter, polygonal but with rounded edges. Under SEM, meshes deep and empty inside (Fig. 7C–F). Processes in the shape of inverted goblets with concave conical trunks and well-defined terminal discs (Figs 6C–F, 7A–F). Terminal discs strongly serrated, with a concave central area (Figs 6C–F, 7B–F). Sparse ultragranulation on the edges of terminal discs visible only under SEM (Fig. 7E–F). Three to five microgranules (0.25–0.30 μm in diameter), covered with ultragranulation, present in the centre of the terminal disc (visible only under SEM; Fig. 7B–F, empty arrowheads).

**Reproductive mode**

The examined population is dioecious (gonochoristic). Males were identified using aceto-orcein staining, which revealed testicles filled with spermatozoa. However, no morphological secondary sexual dimorphism, such as gibbosities on hind legs in males, was identified.

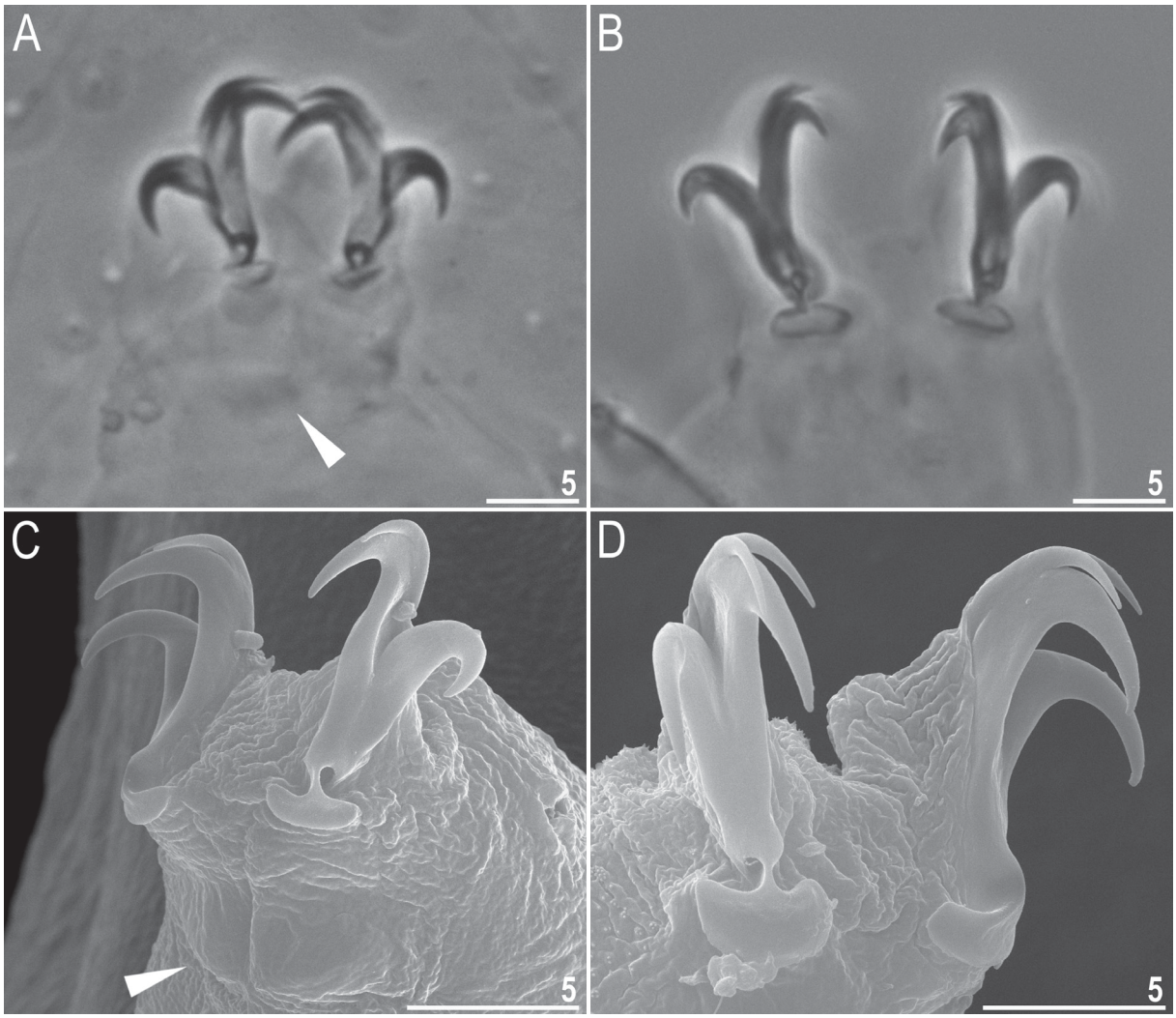


**Fig. 5.** *Macrobiotus canaricus* sp. nov., paratypes, claws. **A–B**. Claws III and IV seen under PCM. **C–D**. Claws I and IV seen under SEM. Arrowheads indicate faint muscle attachments under claws; Figs A and B assembled from several photos. Scale bars in μm.

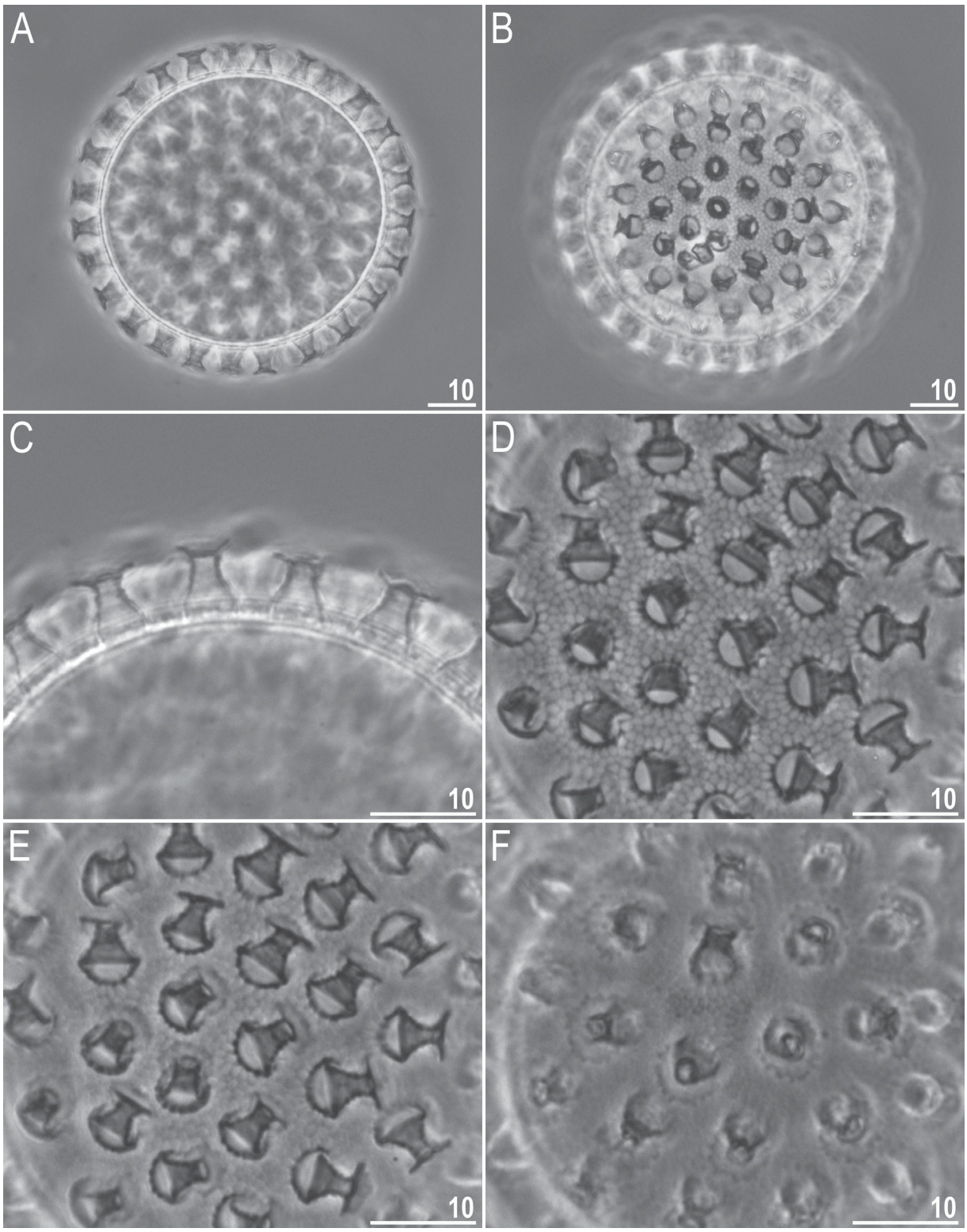


**Fig. 6.** *Macrobiotus canaricus* sp. nov., egg seen under PCM. **A**. Midsection under 400 × magnification. **B**. Surface under 400 × magnification. **C**. Midsection under 1000 × magnification. **D–E**. Surface under 1000 × magnification. **F**. Outlines of terminal discs of egg processes under 1000 × magnification. Scale bars in μm.

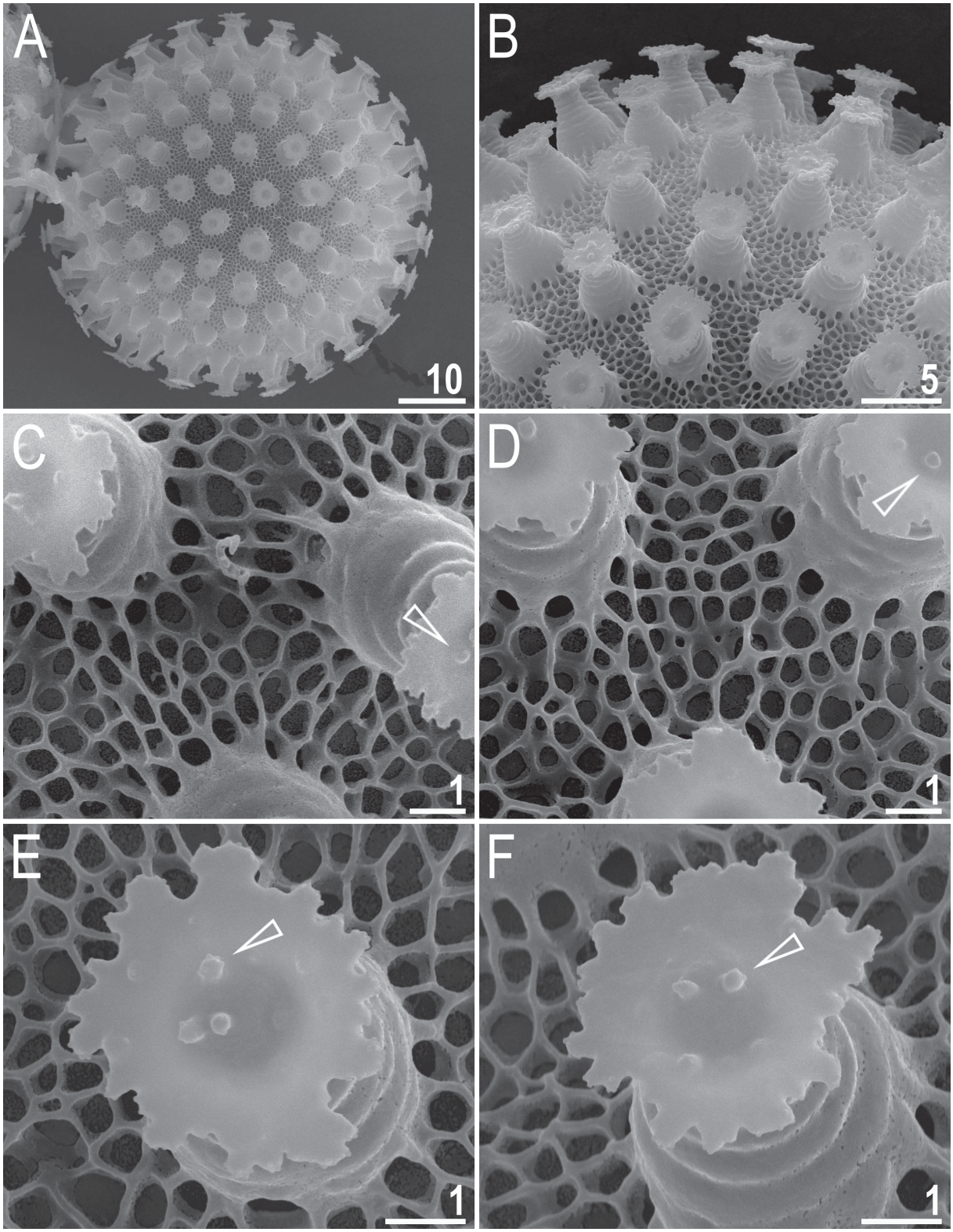


**Fig. 7.** *Macrobiotus canaricus* sp. nov., egg chorion morphology seen under SEM. **A**. Entire egg. **B**. Close up of the egg surface and processes. **C–D**. Details of the egg surface. **E–F**. Details of the terminal discs. Arrowheads indicate granules in the centre of the terminal discs. Scale bars in μm.

**Table 6.** Measurements (in µm) of selected morphological structures of the eggs of *Macrobiotus canaricus* sp. nov. mounted in Hoyer's medium. (N = number of eggs / structures measured; Range = the smallest and the largest structure among all measured specimens; SD = standard deviation)

| Character | N | Range | Mean | SD |
|---|---|---|---|---|
| Egg bare diameter | 30 | 59.9–81.6 | 68.7 | 5.0 |
| Egg full diameter | 30 | 70.2–96.2 | 80.8 | 5.4 |
| Process height | 90 | 3.9–8.2 | 5.5 | 1.0 |
| Process base width | 90 | 3.3–7.5 | 5.3 | 0.8 |
| Process base/height ratio | 90 | 60%–160% | 99% | 19% |
| Terminal disc width | 90 | 3.4–7.5 | 4.8 | 0.8 |
| Inter-process distance | 90 | 1.5–5.5 | 3.4 | 0.8 |
| Number of processes on the egg circumference | 30 | 23–31 | 25.5 | 2.0 |

**DNA sequences**

We obtained sequences for all four of the above-mentioned molecular markers. The two conservative nuclear markers (18S rRNA, 28S rRNA) were represented by single haplotypes, whereas ITS-2 and COI exhibited three and two haplotypes, respectively. The p-genetic distance between the ITS-2 haplotypes ranged from 0.5 to 1.1% and between COI haplotypes it was equal to 1.3%. The 18S rRNA sequence (GenBank: MH063925) was 1033 bp long. The 28S rRNA sequence (GenBank: MH063934) was 721 bp long. The ITS-2 haplotypes 1–3 were 413 bp long (GenBank: MH063928, MH063929 and MH063930, respectively). The COI haplotypes 1–2 were 658 bp long (GenBank: MH057765 and MH057766, respectively).

**Phenotypic differential diagnosis**

By the oral cavity armature of the *maculatus* type and *hufelandi* type of egg shell ornamentation, smooth lunules under claws of all legs and granulation at least on legs IV, the new species is similar to *M. almadai* Fontoura *et al.*, 2008, *M. humilis* Binda & Pilato, 2001, and *M. rawsoni* Horning *et al.*, 1978, but can be differentiated specifically from:

*Macrobiotus almadai*, known only from the Azores (Fontoura *et al.* 2008), by the presence of the external and the internal patch of granulation on legs I–III (legs I–III smooth in *M. almadai*) and by the presence of a single large pore in the centre of the external patch on legs I–III (occasionally, regular cuticular pores may be present on some legs, but such pores are small and never present on all legs in the same place in *M. almadai*).

*Macrobiotus humilis*, reported only from its type locality in Sri Lanka (Binda & Pilato 2001), by the presence of three separated dorsal teeth of the third band (dorsal teeth fused into a single transversal ridge in *M. humilis*), the presence of a subterminal constriction in the second macroplacoid (second macroplacoid without constrictions in *M. humilis*), more posteriorly inserted stylet supports (*pt = 74.3–76.8* in the new species vs *pt = 71.1–71.3* in *M. humilis*), slightly higher pt of the second macroplacoid length (*pt=14.6–19.6* in the new species vs *pt = 12.5–14.4* in *M. humilis*) and by irregularly serrated edges of the terminal discs on egg processes (edges of terminal discs regularly indented in *M. humilis*).

*Macrobiotus rawsoni*, known only from its type locality in New Zealand (Horning *et al.* 1978; Kaczmarek & Michalczyk 2017a), by the presence of granulation on all legs (granulation present only on legs IV in *M. rawsoni*), the presence of a subterminal constriction in the second macroplacoid (second macroplacoid without constrictions in *M. rawsoni*), the absence of cuticular bars under the claws on

legs I–III (thin paired bars present in *M. rawsoni*), more anteriorly inserted stylet supports (*pt = 74.3–76.8* in the new species vs *pt = 77.0–77.1* in *M. rawsoni*), a different morphology of reticulation on the egg surface between processes (several lines of mesh between neighbouring egg processes in the new species vs two lines of mesh between neighbouring egg processes in *M. rawsoni*) and by a smaller mesh size in the chorion reticulum (0.3–1.0 μm in diameter in the new species vs 1.8–2.5 μm in diameter in *M. rawsoni*).

**Genotypic differential diagnosis**

The ranges of uncorrected genetic p-distances between the new species and species of the *Macrobiotus hufelandi* complex, for which sequences are available from GenBank, are as follows:

- **18S rRNA**: 0.5–3.7% (2.0% on average), being most similar to two undetermined species of the *M. hufelandi* group from Spain (FJ435738–9) and to *M. macrocalix* from Poland (MH063926) and the least similar to *M. polypiformis* Roszkowska *et al.*, 2017 from Ecuador (KX810008)
- **28S rRNA**: 1.9–13.2% (6.1% on average), being most similar to three undetermined species of the *M. hufelandi* complex from Spain (FJ435751 and FJ435754–5) and the least similar to *M. polypiformis* from Ecuador (KX810009)
- **ITS-2**: 5.3–27.8% (17.0% on average), with the most similar being *M. macrocalix* from Poland (MH063931) and the least similar being *M. polypiformis* from Ecuador (KX810010)
- **COI**: 17.2–24.7% (19.2% on average), with the most similar being *M. hannae* Nowak & Stec, 2018 from Poland (MH057764) and the least similar being *M. papei* Stec *et al.*, 2018 from Tanzania (MH057763)

***Macrobiotus*** cf. ***recens*** Cuénot, 1932
Figs 8–14, Tables 7–8

**Material examined** (114 animals, 48 eggs)

SPAIN: Canary Islands, Gran Canaria, Presa de Lugarejos, 28°02′38″ N, 15°40′22″ W, 885 m a.s.l., lichen on a stone wall. Specimens mounted on microscope slides in Hoyer's medium (87 animals + 38 eggs), fixed on SEM stubs (8+10), processed for DNA sequencing (4 animals) and used for aceto-orcein staining (15 animals). Slide depositories: 87 animals (slides: ES.006.*, where the asterisk can be substituted by the following numbers 1–4, 10–12, 14–17 ) and 38 eggs (slides: ES.006.*: 5–9, 13) (IZiBB).

**Description of the population from Gran Canaria**

**Animals** (measurements and statistics in Table 7)

Body white in juveniles and slightly yellowish in adults, after fixation in Hoyer's medium transparent (Fig. 8A). Eyes present in live animals and in specimens mounted in Hoyer's medium. Elliptical and sometimes roundish pores (1.0–1.8 μm in diameter), visible under PCM and SEM, scattered randomly on entire body cuticle (Fig. 8B–E), including the external and internal surface of all legs (Fig. 9A–I). Inside pores several granules, visible only under SEM, always present (Fig. 8E). Granulation patch on external and internal surfaces of legs I–III present (Fig. 9A–E). Single pore present at centre of each external granulation patch (Fig. 9A–C). Granulation patch on external surface larger and more distinct than the one on internal surface (Fig. 9A–E). Faint cuticular fold present on external surface of legs I–III just above claws (Fig. 9A–B, empty arrowhead), whereas on internal surface of legs I–III there is a cuticular bulge resembling pulvinus (Fig. 9D–E, filled arrowhead). Both external fold and internal bulge visible only if legs are fully extended and correctly oriented on slide (particularly cuticular fold above claws). Granulation on legs IV always clearly visible and consists of two granulation patches: the distal

**Table 7.** Measurements (in µm) of selected morphological structures of individuals of *Macrobiotus* cf. *recens* Cuénot, 1932 from the Canary Islands mounted in Hoyer's medium. (N = number of specimens / structures measured; Range = the smallest and the largest structure among all measured specimens; SD = standard deviation)

| Character | N | Range | | Mean | | SD | |
|---|---|---|---|---|---|---|---|
| | | µm | *pt* | µm | *pt* | µm | *pt* |
| Body length | 30 | 353–731 | *684–1174* | 576 | *1042* | 66 | *90* |
| Buccopharyngeal tube | | | | | | | |
| Buccal tube length | 30 | 48.5–70.3 | – | 55.4 | – | 5.8 | – |
| Stylet support insertion point | 30 | 39.3–57.2 | *79.1–83.5* | 44.7 | *80.8* | 4.9 | *1.0* |
| Buccal tube external width | 30 | 8.0–15.6 | *15.4–22.8* | 9.8 | *17.6* | 1.6 | *1.4* |
| Buccal tube internal width | 30 | 6.1–12.2 | *11.6–17.8* | 7.5 | *13.4* | 1.3 | *1.3* |
| Ventral lamina length | 30 | 24.9–42.3 | *47.3–63.8* | 32.9 | *59.6* | 3.2 | *4.2* |
| Placoid lengths | | | | | | | |
| Macroplacoid 1 | 30 | 9.4–19.4 | *18.1–30.5* | 13.3 | *24.0* | 2.3 | *2.6* |
| Macroplacoid 2 | 30 | 8.2–17.0 | *15.9–24.8* | 10.6 | *19.0* | 2.0 | *1.8* |
| Microplacoid | 30 | 3.1–8.4 | *5.8–12.3* | 4.7 | *8.5* | 1.1 | *1.3* |
| Macroplacoid row | 30 | 12.5–39.1 | *24.1–57.1* | 25.4 | *45.7* | 5.1 | *6.2* |
| Placoid row | 30 | 17.3–52.6 | *33.4–76.8* | 32.7 | *58.7* | 6.1 | *6.3* |
| Claw 1 lengths | | | | | | | |
| External primary branch | 30 | 12.3–18.0 | *23.1–32.7* | 14.6 | *26.6* | 1.5 | *2.4* |
| External secondary branch | 29 | 9.6–14.6 | *17.9–23.8* | 11.7 | *21.1* | 1.2 | *1.6* |
| Internal primary branch | 30 | 12.0–17.0 | *22.7–29.1* | 14.1 | *25.6* | 1.2 | *1.9* |
| Internal secondary branch | 30 | 8.2–13.7 | *15.7–24.5* | 11.1 | *20.1* | 1.3 | *2.4* |
| Claw 2 lengths | | | | | | | |
| External primary branch | 30 | 12.8–18.3 | *23.2–31.6* | 15.0 | *27.2* | 1.3 | *2.3* |
| External secondary branch | 30 | 8.0–14.6 | *16.5–26.4* | 11.7 | *21.2* | 1.5 | *2.5* |
| Internal primary branch | 30 | 12.0–20.5 | *22.2–39.7* | 14.7 | *26.6* | 1.8 | *3.3* |
| Internal secondary branch | 30 | 8.5–14.9 | *15.5–25.6* | 11.2 | *20.4* | 1.6 | *2.7* |
| Claw 3 lengths | | | | | | | |
| External primary branch | 30 | 13.3–18.2 | *23.9–33.7* | 15.2 | *27.6* | 1.2 | *2.4* |
| External secondary branch | 30 | 8.9–16.2 | *17.2–26.1* | 11.7 | *21.2* | 1.5 | *2.0* |
| Internal primary branch | 30 | 11.1–17.5 | *20.4–32.7* | 14.5 | *26.3* | 1.4 | *2.5* |
| Internal secondary branch | 30 | 9.1–15.1 | *16.7–29.2* | 11.5 | *20.8* | 1.3 | *2.5* |
| Claw 4 lengths | | | | | | | |
| Anterior primary branch | 29 | 11.8–22.2 | *22.6–36.7* | 17.3 | *31.3* | 1.9 | *3.2* |
| Anterior secondary branch | 28 | 11.1–17.2 | *20.6–29.0* | 13.1 | *23.7* | 1.5 | *2.0* |
| Posterior primary branch | 27 | 14.5–23.4 | *28.0–38.9* | 18.1 | *32.7* | 1.6 | *2.5* |
| Posterior secondary branch | 26 | 11.1–17.4 | *20.2–32.0* | 13.7 | *24.6* | 1.6 | *3.1* |

patch with densely distributed granules situated just above claws and the proximal patch being wider with more sparsely distributed granules located immediately above distal patch (Fig. 9G–I).

Mouth antero-ventral. Bucco-pharyngeal apparatus of the *Macrobiotus* type (Fig. 10A–C), with ventral lamina and ten small peribuccal lamellae followed by six buccal sensory lobes. Under PCM, oral cavity armature of the *hufelandi* type, i.e., with all three bands of teeth always visible (Fig. 10B–C). First band of teeth composed of numerous very small cones arranged in four to six rows situated anteriorly in oral cavity, just behind bases of peribuccal lamellae (Figs 10B–C, 11A–B, filled arrowhead). Second band of teeth situated between ring fold and third band of teeth and comprises 4–5 rows of small cones, slightly larger than those of first band (Figs 10B–C, 11A–B, empty arrowhead). Teeth of the third band located within posterior portion of oral cavity, between the second band of teeth and buccal tube

opening (Figs 10B–C, 11A–B). Third band of teeth discontinuous and divided into dorsal and ventral portions. Under PCM, dorsal teeth seen as three distinct transversal ridges, whereas ventral teeth appear as two separate lateral transversal ridges and a roundish median tooth (Fig. 10B–C). Under SEM, both dorsal and ventral teeth clearly distinct (Fig.11A–B). Medio-ventral tooth rarely divided into two or three smaller teeth (Fig. 11B). Under SEM, margins of dorsal and latero-ventral teeth slightly serrated (Fig. 11A–B). Pharyngeal bulb spherical, with triangular apophyses, two rod-shaped macroplacoids and

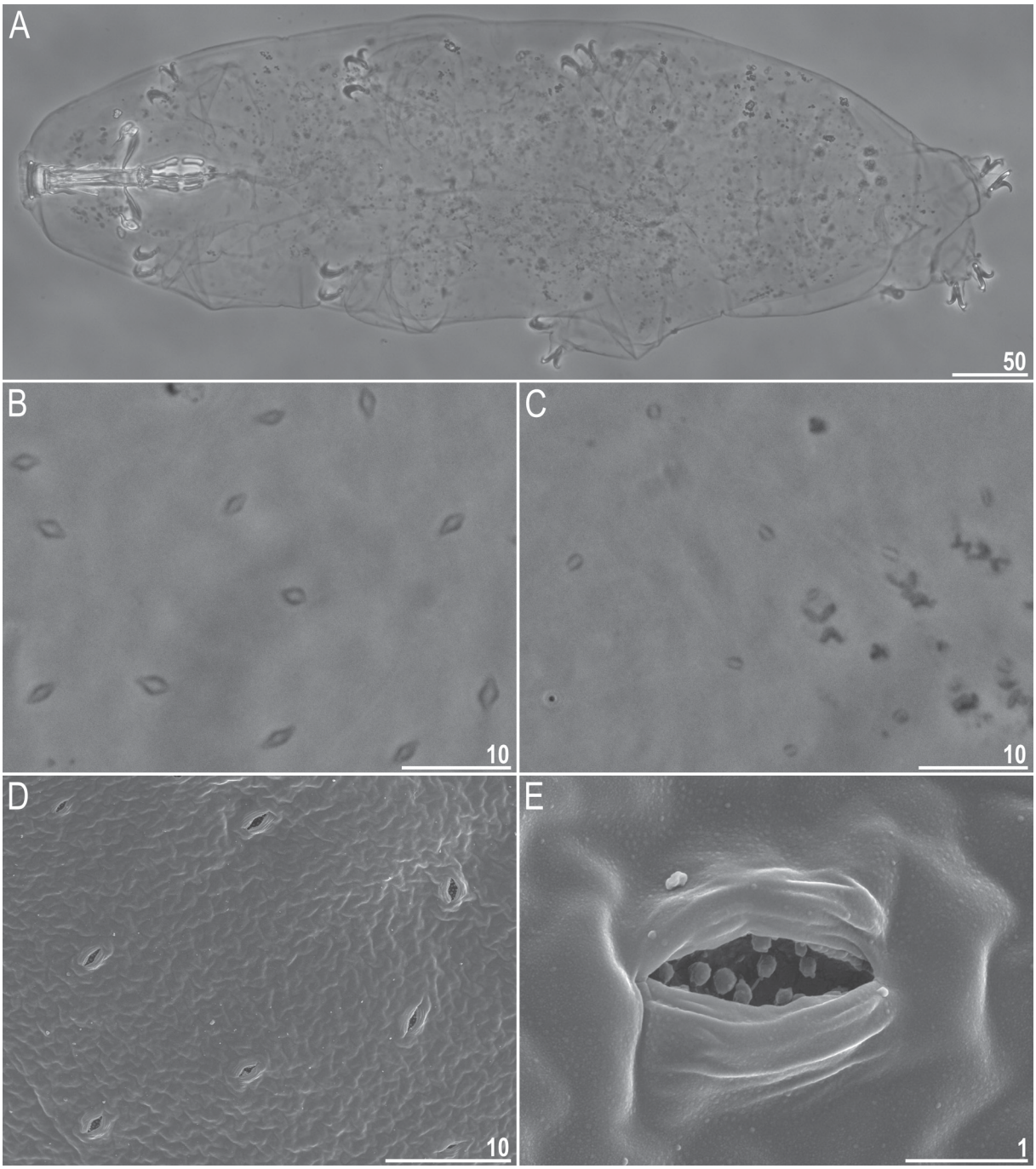


**Fig. 8.** *Macrobiotus* cf. *recens* Cuénot, 1932*,* Gran Canaria, habitus and cuticular pores. **A**. Dorso-ventral projection (PCM). **B–C**. Pores on the dorsal and ventral cuticle, respectively (PCM). **D**. Pores on the dorsal cuticle (SEM). **E**. Granulation inside a single pore (SEM). Scale bars in μm.

one big rod-shaped microplacoid (Fig. 10D–E). Macroplacoid length sequence 2 < 1. First and second macroplacoid with the central and the subterminal constriction, respectively (Fig. 10D–E).

Claws Y shaped, of the *hufelandi* type (Fig. 12A–D). Primary branches with distinct accessory points and with an evident stalk connecting claw to lunula (Fig. 12A–D). Lunulae I–III smooth (Fig. 12A, C), whereas lunulae IV slightly crenulated (Fig. 12B, D). Faint cuticular bars under claws I–III present, more visible in larger specimens (Fig. 12A, C). Horseshoe-shaped structure connects anterior and posterior lunules (Fig. 12B).

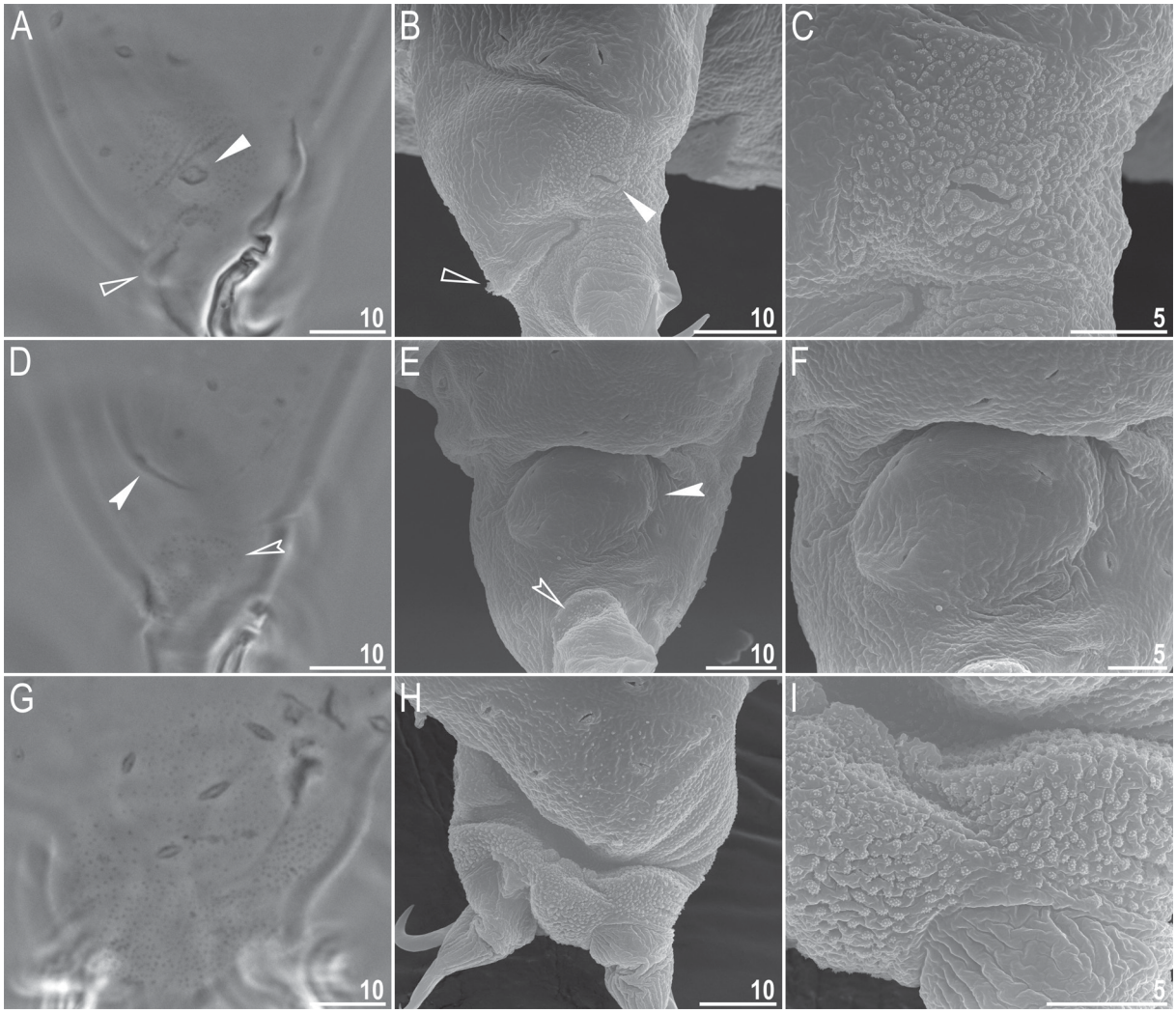


**Fig. 9.** *Macrobiotus* cf. *recens* Cuénot, 1932*,* Gran Canaria, structures on forelegs seen under PCM and under SEM. **A–C**. The patch of granulation on the external surface of leg II, with the cuticular pore at the centre of the patch and the cuticular fold above the claws. **D**–**F**. The patch of granulation and the cuticular bulge (pulvinus) on the internal surface of leg III. **G–I**. Granulation on leg IV. Filled flat arrowheads indicate the large pore at the centre of the external granulation patch, empty flat arrowheads indicate the cuticular fold above the claws on the external leg surface, filled indented arrowheads indicate the cuticular fold (pulvinus) on the internal leg surface, and empty indented arrowheads indicate granulation on the internal leg surface. Scale bars in μm.

**Eggs** (measurements and statistics in Table 8)
Laid freely, white/light yellow, spherical or slightly oval (Figs 13A–B, 14A). Surface between processes of the *hufelandi* type, i.e., chorion surface between processes covered by reticulum with very small meshes (Figs 13C–D, 14B–E). Under PCM, surface between processes seems to be covered by dark dots (Fig. 13C) and only sometimes a clear reticulation is visible (Fig. 13D). Several rows of meshes between egg processes (usually 7–8). Mesh borders and nodes/knots thick and sometimes wider than mesh diameter (Fig. 14B–E). Meshes circular or slightly oval (0.4–0.9 μm in diameter) and under SEM

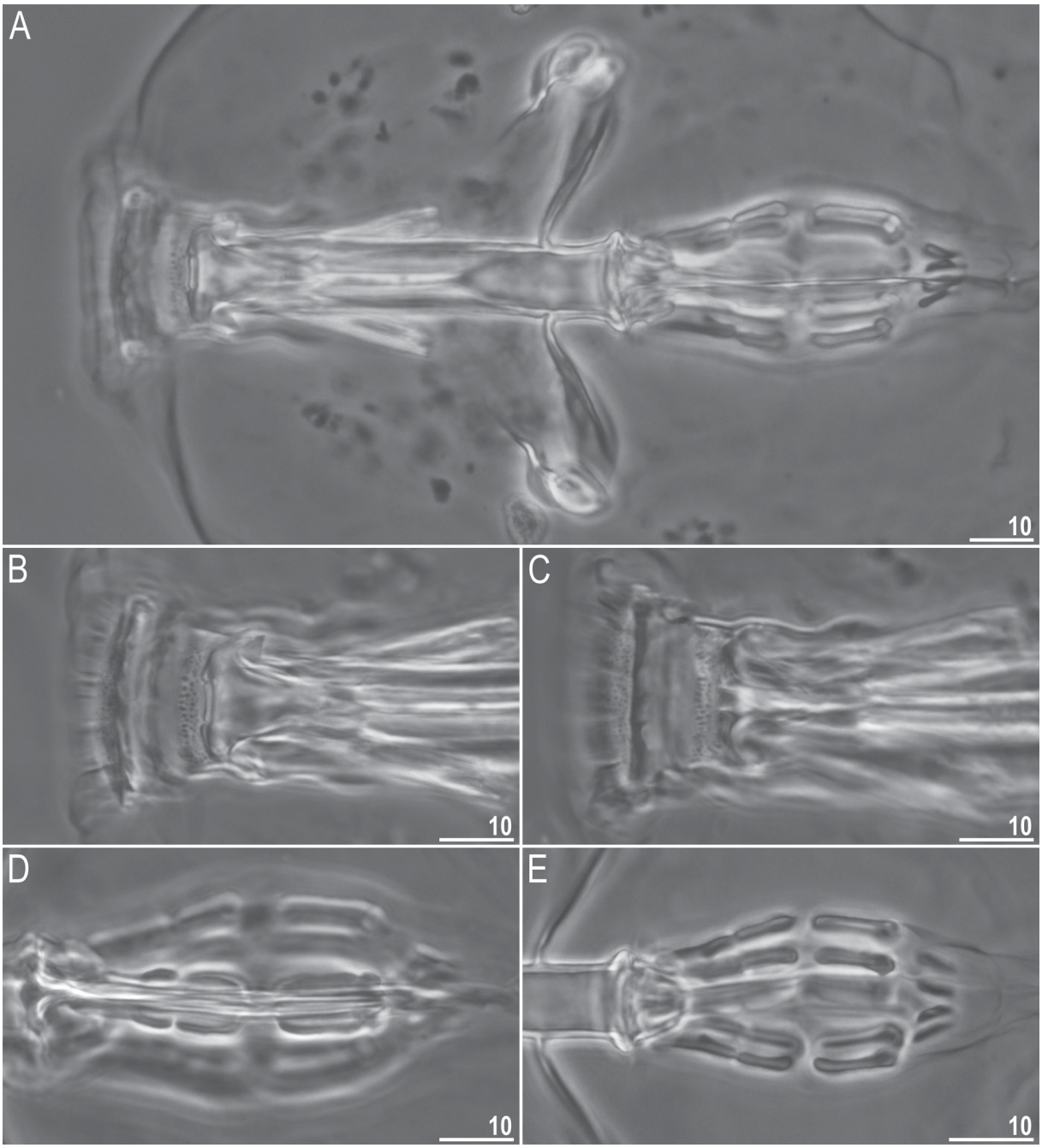


**Fig. 10.** *Macrobiotus* cf. *recens* Cuénot, 1932, Gran Canaria, buccal apparatus and the oral cavity armature seen under PCM. **A**. Dorsal projection of the entire buccal apparatus. **B–C**. Dorsal and ventral view of the oral cavity armature, respectively. **D–E**. Placoid morphology. Scale bars in μm.

**Table 8.** Measurements (in µm) of selected morphological structures of the eggs of *Macrobiotus* cf. *recens* Cuénot, 1932 from the Canary Islands mounted in Hoyer's medium. (N = number of eggs/structures measured; Range = the smallest and the largest structure among all measured specimens; SD = standard deviation)

| Character | N | Range | Mean | SD |
|---|---|---|---|---|
| Egg bare diameter | 30 | 86.1–113.7 | 102.1 | 8.0 |
| Egg full diameter | 30 | 113.6–151.4 | 137.6 | 9.3 |
| Process height | 90 | 13.4–26.3 | 20.0 | 2.7 |
| Process base width | 90 | 3.2–10.7 | 6.3 | 1.4 |
| Process base/height ratio | 90 | 16%–45% | 32% | 6% |
| Inter-process distance | 90 | 3.7–74.0 | 6.6 | 7.3 |
| Number of processes on the egg circumference | 30 | 21–27 | 24.6 | 1.5 |

all pores empty inside (Fig. 14C–D). Mesh diameter decreases gradually from peribasal to interbasal meshes (Fig. 14C–D). Short thickenings radiating from process bases are often visible under PCM and always visible under SEM; thickenings may create a crown around process bases (Figs 13C, 14C–D, filled arrowheads). Processes in the shape of high and thin cones with straight conical trunks, devoid of terminal discs and sometimes bifurcated (Figs 13A–F, 14A–F). Trunks of processes slightly undulated. Undulations covered by numerous granules composed of microgranule aggregations. Undulations and granules poorly visible under PCM (Fig. 13C–F). Undulations, granules and microgranules always clearly visible under SEM (Fig. 14B, E–F).

**Reproductive mode**

The examined population is dioecious (gonochoristic). Males were identified using aceto-orcein staining, which revealed testicles filled with spermatozoa. However, no morphological secondary sexual dimorphism, such as gibbosities on hind legs in males, was identified.

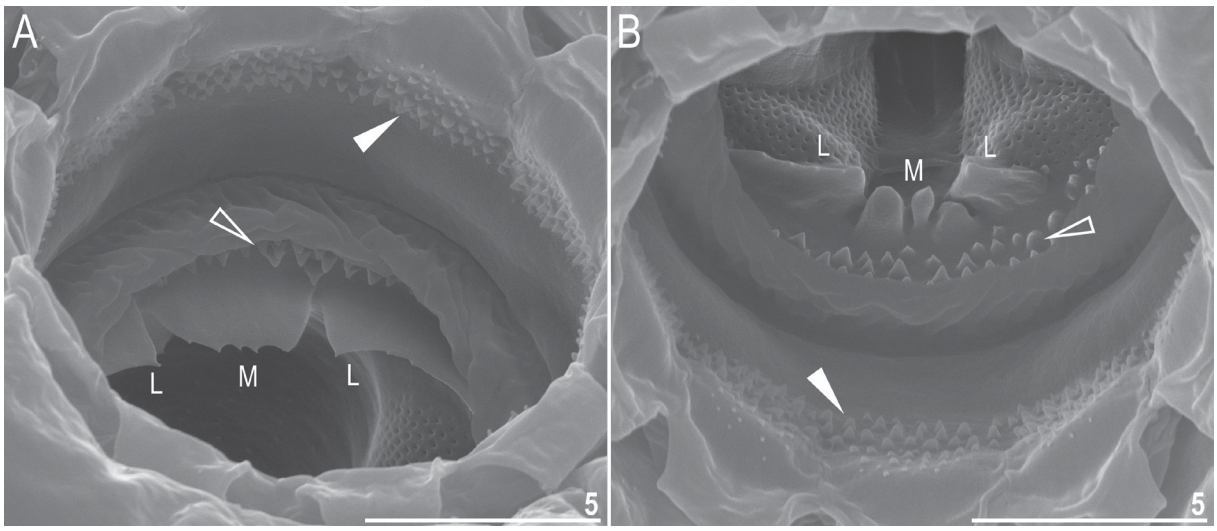


**Fig. 11.** *Macrobiotus* cf. *recens* Cuénot, 1932*,* Gran Canaria, oral cavity armature seen under SEM from different angles. **A**. View of the dorsal portion. **B**. View of the ventral portion. Filled arrowheads indicate the teeth of the first band, empty arrowheads indicate the teeth of the second band, median teeth are marked with M, and lateral teeth are marked with L. Scale bars in µm.

**DNA sequences**

We obtained sequences for all four of the above-mentioned molecular markers. The two conservative nuclear markers (18S rRNA, 28S rRNA) were represented by single haplotypes, whereas both ITS-2 and COI exhibited two haplotypes. The p-genetic distance between the ITS-2 as well as between the COI haplotypes was 1.1%. The 18S rRNA sequence (GenBank: MH063927) was 1033 bp long, the 28S rRNA sequence (GenBank: MH063936) was 725 bp long, the ITS-2 haplotype 1 and 2 sequences (GenBank: MH063932 and MH063933, respectively) were 420 bp long; the COI haplotype 1 and 2 sequences (GenBank: MH057768 and MH057769, respectively) were 658 bp long.

**Genotypic differential diagnosis**

The ranges of uncorrected genetic p-distances between the new species and species of the *Macrobiotus hufelandi* complex, for which sequences are available from GenBank, are as follows:

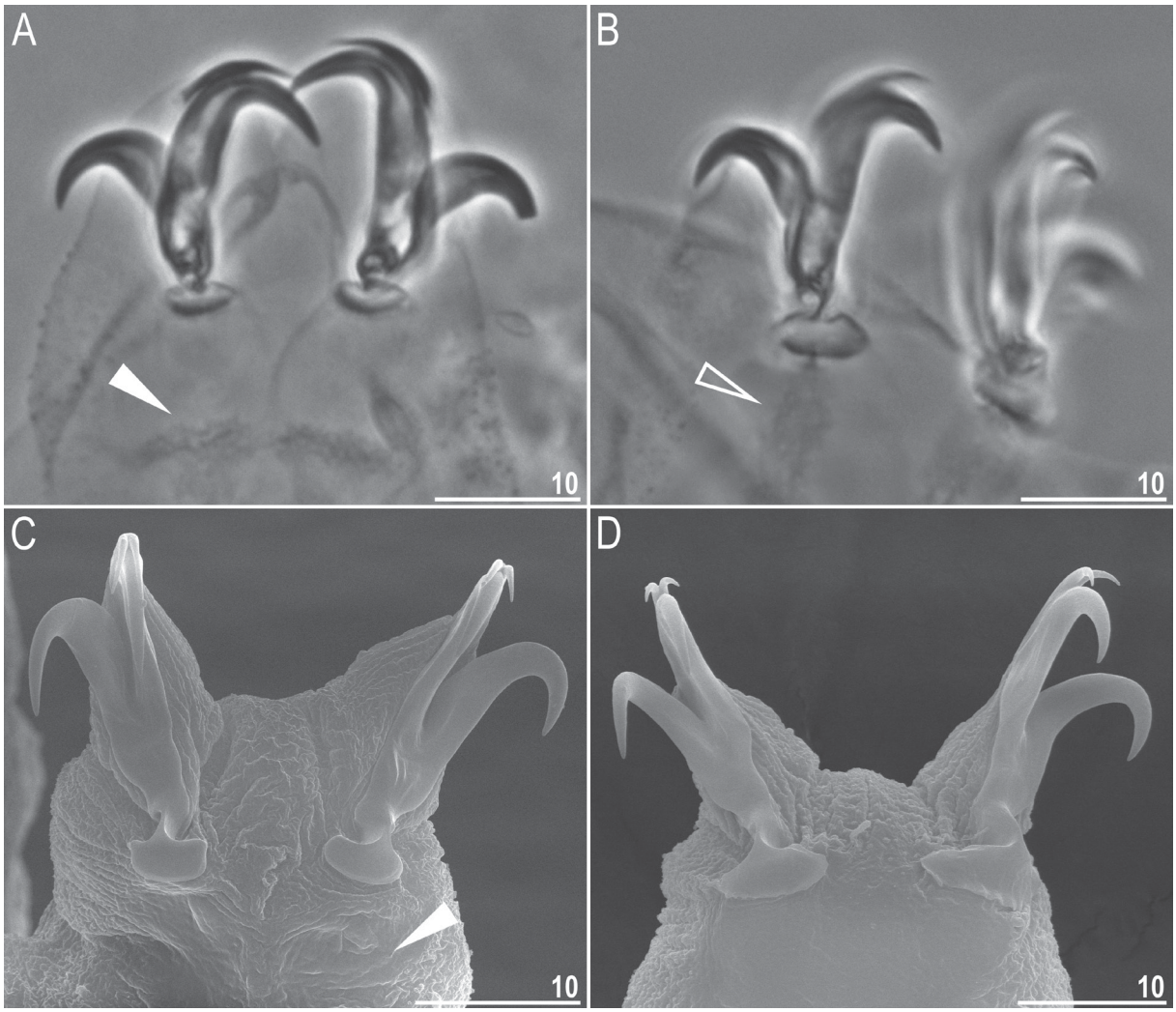


**Fig. 12.** *Macrobiotus* cf. *recens* Cuénot, 1932*,* Gran Canaria, claws. **A–B**. Claws III and IV seen under PCM, with smooth and weakly crenulated lunules, respectively. **C–D**. Claws II and IV seen under SEM, with smooth and weakly crenulated lunules, respectively. A and B assembled from several photos. Filled arrowheads indicate faint cuticular bars under claws whereas empty arrowhead indicates a horseshoe-shaped structure. Scale bars in μm.

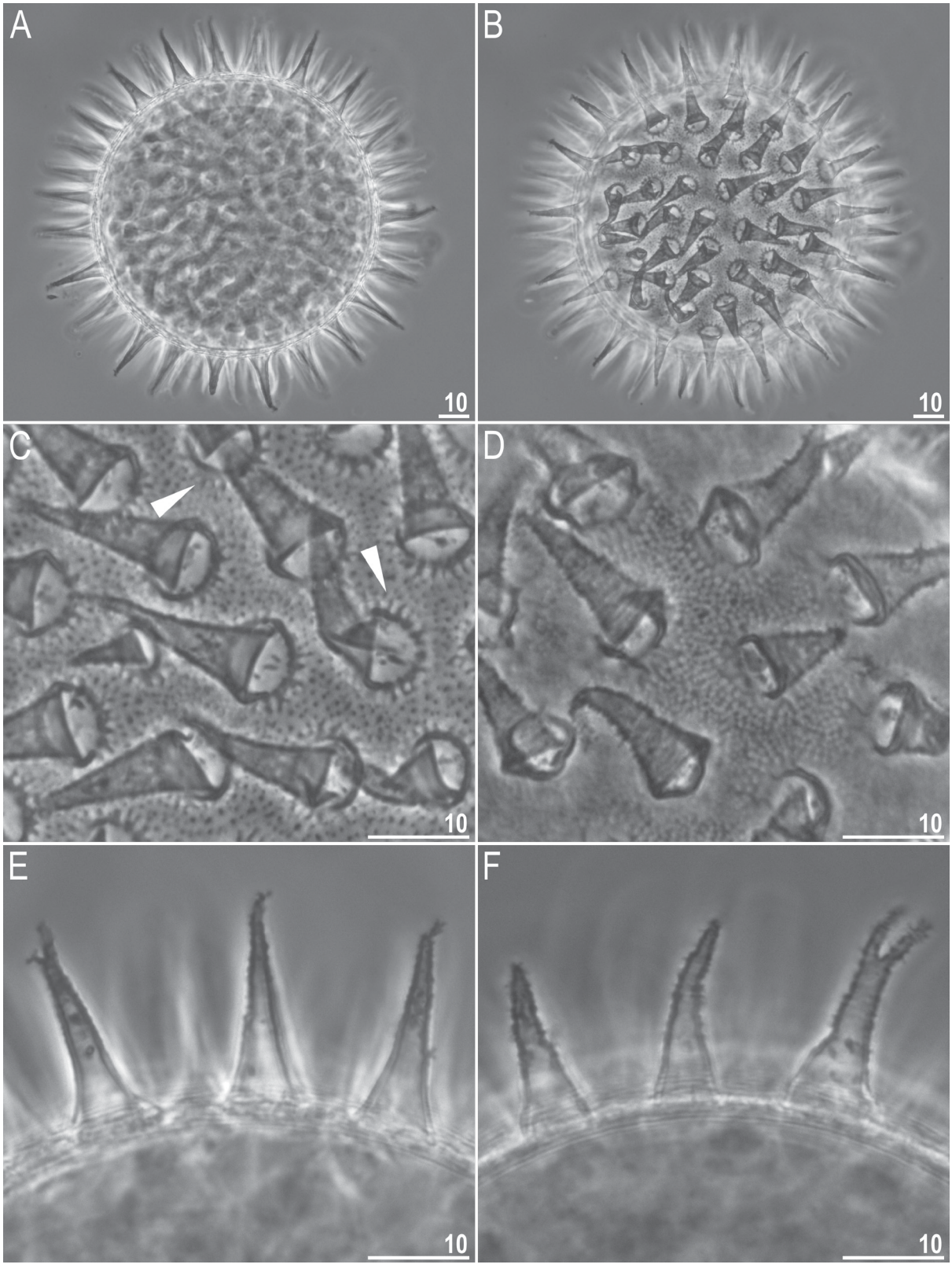


**Fig. 13.** *Macrobiotus* cf. *recens* Cuénot, 1932*,* Gran Canaria, egg seen under PCM. **A**. Midsection under 400 × magnification. **B**. Surface under 400 × magnification. **C–D**. Surface under 1000 × magnification. **E–F**. Midsection under 1000 × magnification. Filled arrowheads indicate short thickenings radiating from the processes bases. Scale bars in μm.

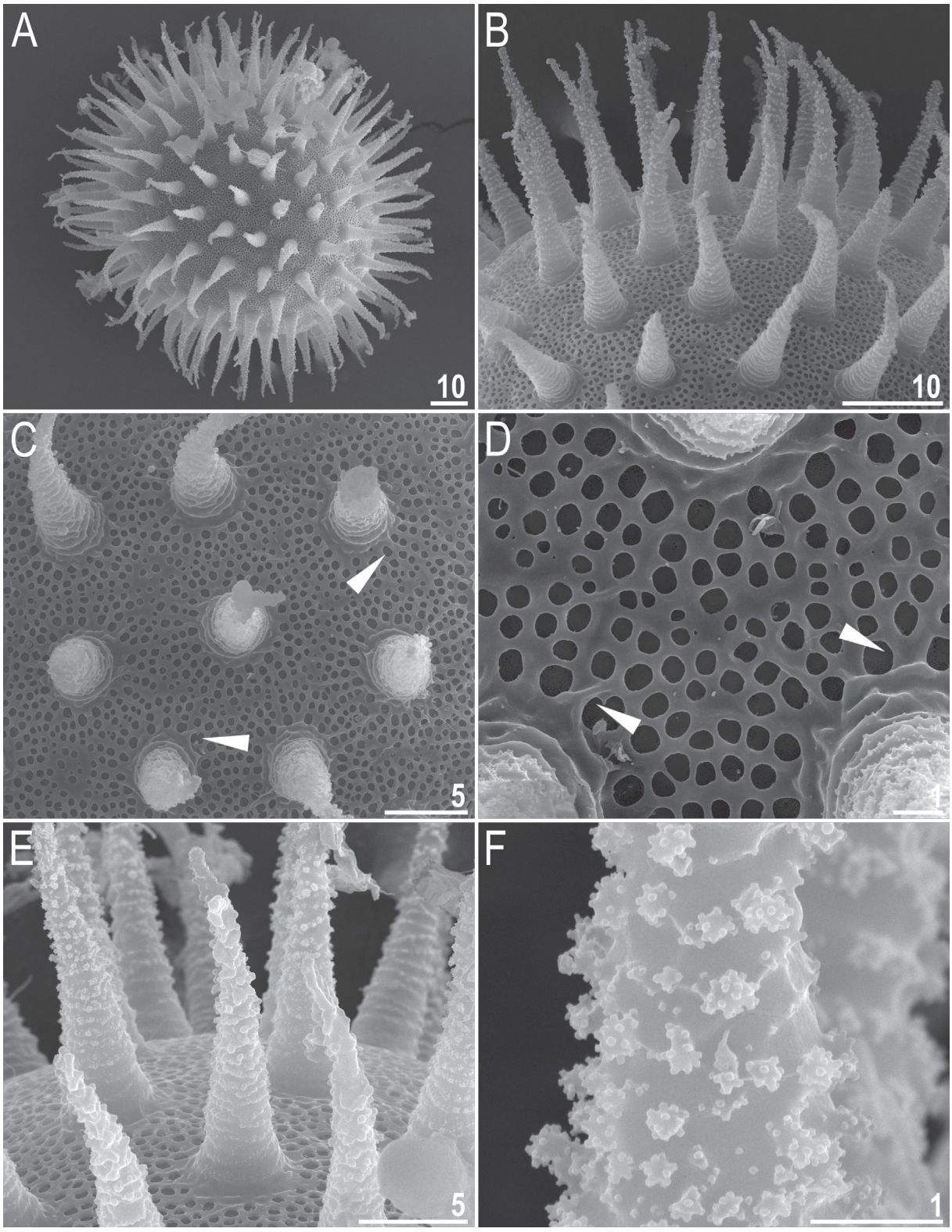


**Fig. 14.** *Macrobiotus* cf. *recens* Cuénot, 1932, Gran Canaria, egg chorion morphology seen under SEM. **A**. Entire egg. **B**. Close up of the egg surface and processes. **C–D**. Details of the egg surface. **E–F**. Details of process morphology. Filled arrowheads indicate short thickenings radiating from the process bases. Scale bars in μm.

- **18S rRNA**: 0.4–4.0% (2.0% on average), with the most similar being *M. macrocalix* from Poland (MH063926) and the least similar being *M. polypiformis* from Ecuador (KX810008)
- **28S rRNA**: 1.3–13.6% (6.5% on average), with the most similar being *M. macrocalix* from Poland (MH063935) and the least similar being *M. polypiformis* from Ecuador (KX810009)
- **ITS-2**: 3.7–26.7% (16.9% on average), with the most similar being *M. macrocalix* from Poland (MH063931) and the least similar being *M. polypiformis* from Ecuador (KX810010)
- **COI**: 16.4–24.7% (19.1% on average), with the most similar being *M. macrocalix* from Italy (FJ176203–7 and FJ176213–7) and the least similar being *M. papei* from Tanzania (MH057763)

**Molecular phylogeny**

Phylogenetic analyses conducted on macrobiotid 18S rRNA sequences as well as on the concatenated macrobiotid data set unambiguously confirmed that the two studied species represent the *M. hufelandi* group (Figs 15–16). The phylogeny based on the COI sequences of the *hufelandi* group also corroborated these results, since none of the two species were recovered external to the species of the *hufelandi* group (Fig. 17). In all analyses, two clades within the *hufelandi* group were present, although the species composition varied slightly between phylogenies based on different markers. One clade grouped exclusively species that exhibit modified egg processes (*M. paulinae* Stec *et al.*, 2015, *M. polypiformis*, *M. papei*, *M. shonaicus* Stec *et al.*, 2018a, *M. scoticus* Stec *et al.*, 2017b and *M. kristenseni* Guidetti, Peluffo, Rocha, Cesari & Moly de Peluffo, 2013); 'the *kristenseni* clade' henceforth. The other clade comprised mostly species with typical inverted goblet-shaped egg processes ('the *hufelandi* clade' hereafter). In contrast to our predictions, *M.* cf. *recens*, with its atypical egg processes, was always embedded within the *hufelandi* clade. The two clades were well supported in phylogenies based on the concatenated data set and on COI sequences, but weakly supported in the 18S rRNA tree (Figs 15–17). Moreover, in the 18S rRNA analysis the *kristenseni* clade, in addition to the majority of species with modified egg processes, comprised *M. sapiens* Binda & Pilato, 1984 (DQ839601) and undetermined species of the *M. hufelandi* group (HQ604971), of which at least the first species exhibits the typical egg morphology. In contrast to other analyses, the 18S rRNA phylogeny recovered a clade, with *X. pseudohufelandi* (Iharos, 1966) and *M. polonicus* Pilato, Kaczmarek, Michalczyk & Lisi, 2003, that was in a sister relationship to all other species of the *hufelandi* group, suggesting that the *hufelandi* group is polyphyletic or that *Xerobiotus* belongs to the *hufelandi* group (Fig. 15).

## Discussion

Thanks to the detailed morphological and molecular analyses, we were able to describe a new species *M. canaricus* sp. nov. and characterise a population of *M.* cf. *recens*, both collected on the Canary Islands. Moreover, by the use of phylogenetic inference, we confirmed the affinity of both studied species with the *M. hufelandi* group.

*Macrobiotus recens* was described in 1932 by Lucien Cuénot, but soon after, some researchers started questioning the status of this species and classified it as '*M. hufelandi* forma *recens*' (Marcus 1936; Ramazzotti 1945, 1962, 1972; Rudescu 1946; Grigarick *et al.* 1973). However, Maucci (1979) analysed several Portuguese populations he identified as *M. recens* morphologically and confirmed that the taxon is indeed a 'bona species'. However, it should be noted that the locus typicus for *M. recens* is La Tardière, a commune in the Vendée department, in the Pays de la Loire region in western France. Thus, similarly to our study, the comparison presented by Maucci (1979) has to be treated with caution, as it may be based on a related species rather than *M. recens* s.str. Since the original description is outdated and incomplete, a confident identification of *M. recens* is currently not possible. Although Pilato & Bertolani (2004) supported the identification of the Portuguese populations studied by Maucci (1979) as *M. recens*, we think that without an integrative redescription of the species it is not possible to test whether *M. recens* is a single species or a complex of morphologically similar taxa. Thus, instead of designating the Canary

Islands population as *M. recens*, we treat it as *M.* cf. *recens*, at the same time highlighting the need for a redescription based on new material from the locus typicus. It could be hypothesised that our Canarian population, as well as previous records of *M. recens* outside the type locality, i.e., from Romania (Rudescu 1946), Italy (Ramazzotti 1945), Greece (Marcus 1936), Portugal (Maucci 1979) and China (Rahm 1937; Bartoš 1963), may represent distinct taxa that could become identifiable only after a modern redescription of *M. recens*. This would not be surprising, as such a pattern has been observed before, for example, when nominal taxa in other groups were described: *Macrobiotus hufelandi* (redescribed by Bertolani & Rebecchi 1993 and Bertolani *et al.* 2011a), *Milnesium tardigradum* (redescribed by Michalczyk *et al.* 2012), *Mesocrista spitsbergensis* (redescribed by Gąsiorek *et al.* 2016), *Hypsibius dujardini* (redescribed by Gąsiorek *et al.* 2018) or *Ramazzottius oberhaeuseri* (redescribed by Stec *et al.* 2018c). Thus, in our

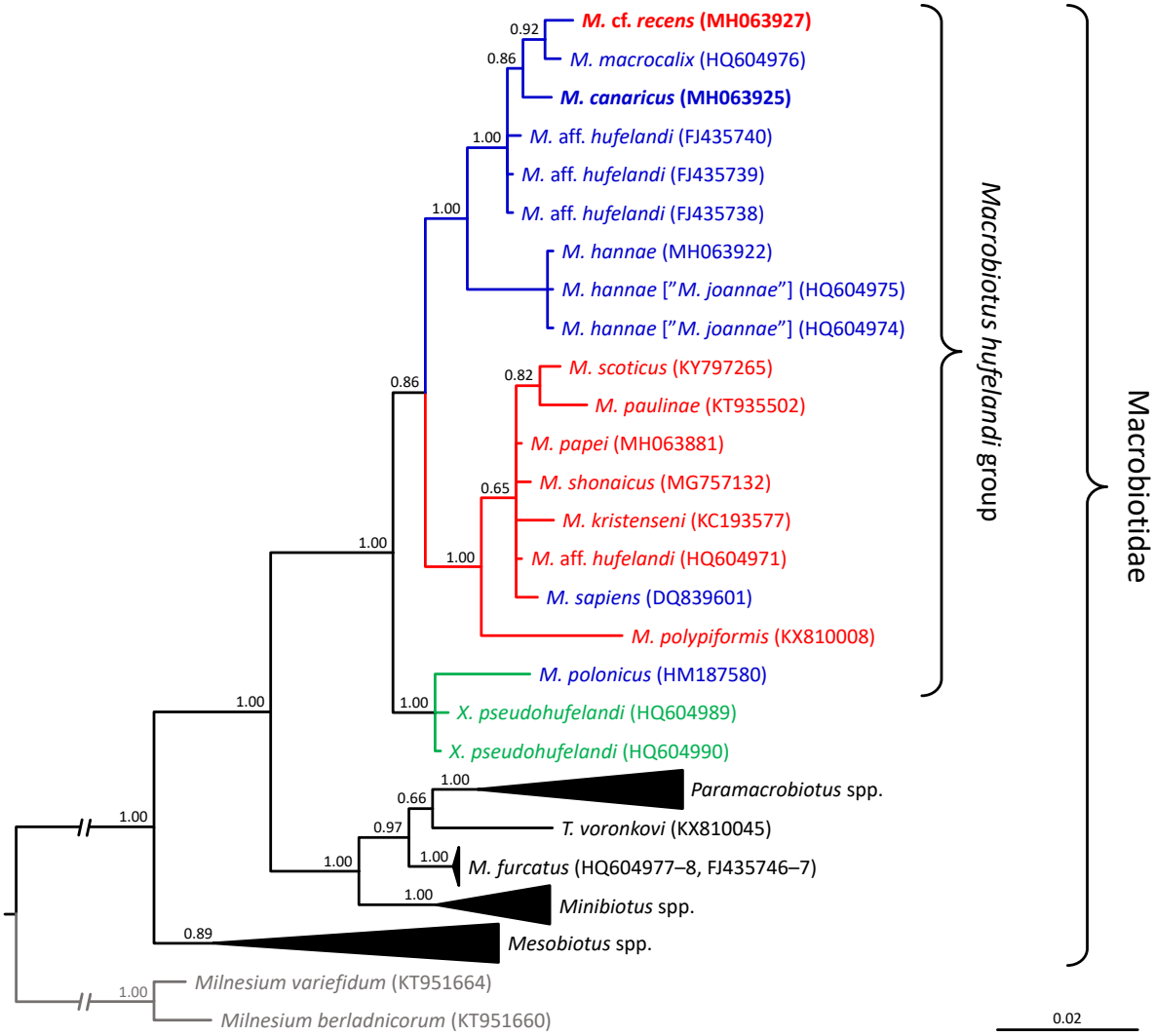


**Fig. 15.** The Bayesian Inference (BI) phylogeny constructed from 18S rRNA sequences of the family Macrobiotidae. Numbers at nodes indicate the Bayesian posterior probability. Species of the *hufelandi* group with typical and atypical egg processes are indicated by blue and red fonts, respectively. The *X. pseudohufelandi* + *M. polonicus* clade, which is in a sister relationship to all other species of the *hufelandi* group, is indicated by green branches. See Table 2 and the Phylogenetic analysis subsection in Material and methods for details on species sequences used in the analysis. The remaining macrobiotids are marked with black and the outgroup is marked with grey. Scale bar represents substitutions per position.

opinion, all records of *M. recens* outside its type locality should be considered as uncertain identifications until a redescription of *M. recens* is available and at least some of the reports can be verified. Following this logic, if the record of *M.* cf. *recens* from the Canary Islands turns out to represent *M. recens* s.str., then this study will be an addition to our poor knowledge of the intraspecific variability in tardigrades. If, however, the current record represents a new species, then, with the data already presented in our study, only a new name will have to be proposed to erect a new species.

Recently, Stec *et al.* (2018a) showed two well supported COI lineages within the *M. hufelandi* group: one clade grouping species with *hufelandi*-type egg processes in the shape of inverted goblets, and the other with modified egg process (conical processes or processes with filaments growing out of terminal discs). Thus, *M.* cf. *recens*, with its conical egg processes, should be expected to cluster with species with modified egg processes. However, in contrast to this prediction, *M.* cf. *recens* is embedded within the clade with species exhibiting typical egg morphology in our COI analysis (Fig. 17). Moreover, the

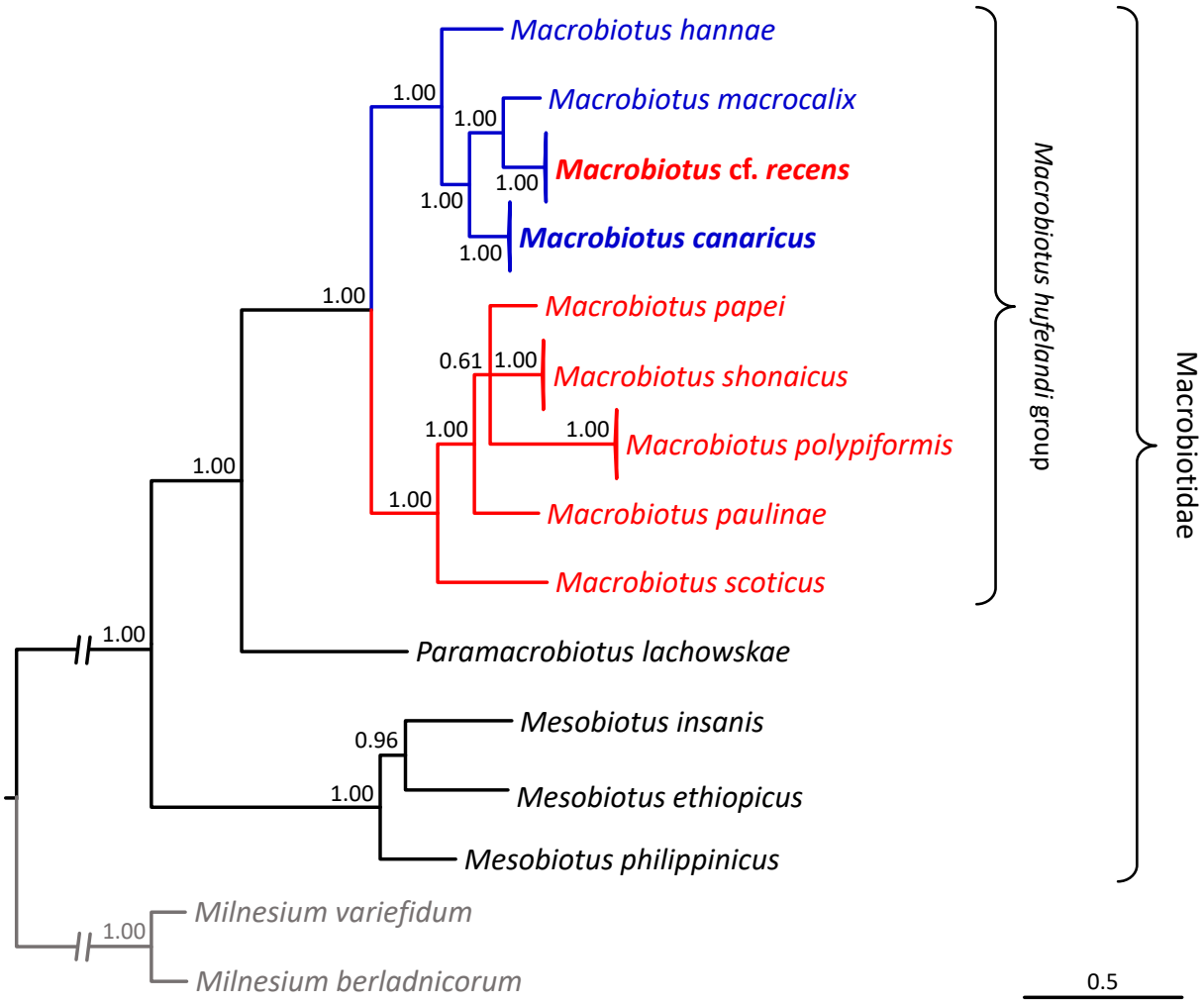


**Fig. 16.** The Bayesian Inference (BI) phylogeny constructed from concatenated sequences (18S rRNA + 28S rRNA + ITS-2 + COI) of the family Macrobiotidae. Numbers at nodes indicate the Bayesian posterior probability. Species of the *hufelandi* group with typical and atypical egg processes are indicated by blue and red fonts, respectively. See Table 2 and the Phylogenetic analysis subsection in Material and methods for details on the species sequences used in the analysis. The remaining macrobiotids are marked with black and the outgroup is marked with grey. The scale bar represents substitutions per position.

same position of the species was recovered in the 18S rRNA phylogeny (Fig. 15) and in the analysis based on four concatenated markers (Fig. 16). Also, *M. sapiens*, with typical egg processes, should be present in the *hufelandi* clade, but in our analyses it clustered with species exhibiting mostly modified processes (Fig. 15). Importantly, however, the 18S rRNA sequence identified as *M. sapiens* (DQ839601; Schill & Steinbrück 2007) comes from Croatia, whereas the type locality of the species is in Sicily (Binda & Pilato 1984). Thus, given that there are no type/neotype sequences for *M. sapiens* and Schill & Steinbrück (2007) did not provide SEM photomicrographs of Croatian eggs, it is not possible to verify the identity of the DQ839601 sequence. In other words, the sequence may represent a similar species of the *hufelandi* group that may exhibit terminal disc filaments. Nevertheless, regardless of the phylogenetic position of *M. sapiens*, the affinity of *M.* cf. *recens* with species exhibiting typical egg processes shows that the morphological criterion proposed by Stec *et al.* (2018a) to distinguish the two clades is not

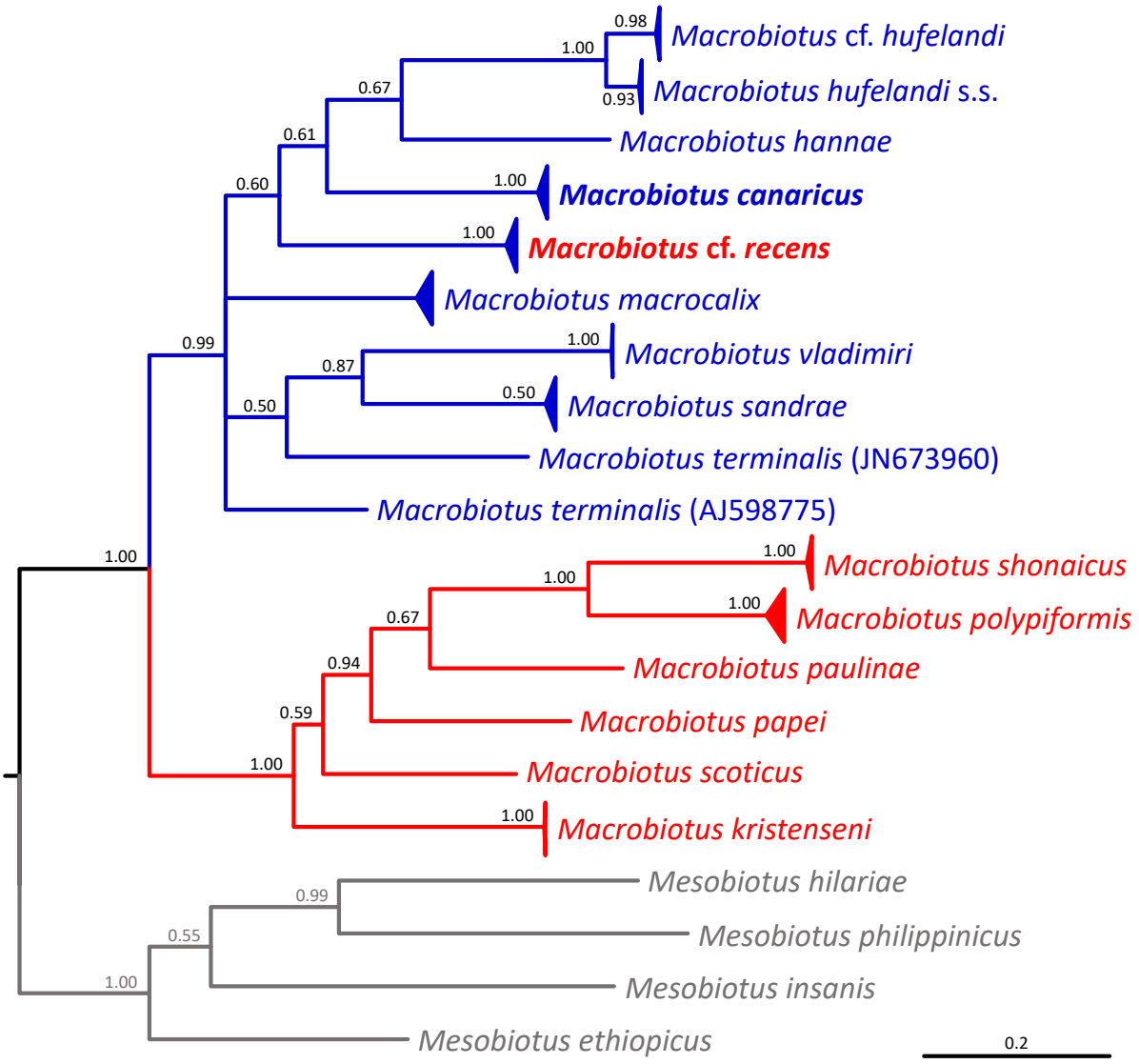


**Fig. 17.** The Bayesian Inference (BI) phylogeny constructed from COI sequences of the species of the *Macrobiotus hufelandi* group. Numbers at nodes indicate the Bayesian posterior probability. Species of the *hufelandi* group with typical and atypical egg processes are indicated by blue and red fonts, respectively. See Table 2 for details on the species sequences used in the analysis. The outgroup is marked with grey. The scale bar represents substitutions per position.

universal. Therefore, more species representing the two clades need to be sequenced to elucidate the taxonomic status of the two clades.

Another species whose phylogenetic position diverges from the predicted is *M. polonicus*. This species, with typical egg processes, should be embedded within the *hufelandi* clade. However, in the 18S rRNA phylogeny, not only does it not cluster within the *hufelandi* clade, but it clusters with *Xerobiotus pseudohufelandi* in a clade that is in a sister relationship to the entire *hufelandi* group. The *M. polonicus* + *X. pseudohufelandi* clade was also found to be a sister group to all other *hufelandi* group species by Bertolani *et al.* (2014). The genus *Xerobiotus* Bertolani & Biserov, 1996 shares a similar morphology of the buccal apparatus, egg shell and spermatozoa with species of the *M. hufelandi* group, but it differs from them by having strongly reduced claws. Given that the *M. polonicus* + *X. pseudohufelandi* clade contains only a single *hufelandi* group sequence, the clade could be a statistical artefact or possibly the 18S rRNA marker is too conservative to solve the relationships between the *hufelandi* group and the genus *Xerobiotus*. Therefore, it is crucial to analyse more populations of *M. polonicus*, other species of the *persimilis* subgroup (*sensu* Kaczmarek & Michalczyk 2017b) and species of the genus *Xerobiotus*, both in terms of the 18S rRNA marker and additional, more variable DNA fragments. If, however, more species of the *hufelandi* group turn out to cluster with the genus *Xerobiotus*, then the taxonomic status of the genus and of the *hufelandi* group should be reconsidered.

Although our multilocus phylogeny supports the presence of two distinct evolutionary lineages within the *hufelandi* group, the taxon sample size is still very low and more precise conclusions concerning the phylogeny of the group cannot currently be made. Thus, to provide more reliable conclusions, much more effort should be made to obtain multilocus molecular data linked to morphology for a larger number of species and populations. Particularly, it would be beneficial to increase the sample size, both in terms of markers as well as species, for the *M. polonicus* + *X. pseudohufelandi* clade to test whether the genus *Xerobiotus* and the *hufelandi* group are monophyletic. Another clade which would benefit from an increased sample size is the clade that comprises species with modified egg processes. Currently, the clade consists of species with two very different process morphotypes, i.e., species having processes with flexible filaments on the terminal discs and species having conical processes devoid of terminal discs. Thus, it might be possible that increased sampling could reveal the presence of two further clades that differ by the egg process morphology. Nevertheless, our findings support the previous results that egg morphology seems to be evolving faster than animal morphology, which underlines the usefulness of chorion ornamentation in the delineation of closely related species (Guidetti *et al.* 2013; Stec *et al.* 2016a, 2017a, 2018a).

## Acknowledgments

We are grateful to Marta Kapała for collecting the samples on the Canary Islands. We would also like to thank Professor Paulo Fontoura (University of Porto, Portugal) for lending us slides with *M. almadai* and to Matteo Vecchi (University in Modena, Italy), who kindly sent us the photos of specimens and eggs from Portugal identified by Maucci (1979) as *M. recens* and deposited in the Maucci collection. We are also grateful to Matteo Vecchi and an anonymous reviewer, whose comments helped to improve our work. We would like to thank the Aquatic Ecosystems Team from the Institute of Environmental Sciences (Jagiellonian University, Kraków) for providing us with the rotifers. The study was supported by the Linnean Society of London and the Systematics Association (a grant from the Systematics Research Fund awarded to DS) and by the Jagiellonian University (subsidy no. K/ZDS/007357 to ŁM).

## References

Bartoš E. 1963. Die Tardigraden der chinesischen und javanischen Moosproben. *Acta Societatis Zoologicae Bohemoslovenicae* 27: 108–114.

Bertolani R. 1971. Rapporto-sessi e dimorfismo sessuale in *Macrobiotus* (Tardigrada). *Rendiconti Accademia Nazionale Lincei* 50 (8): 377–382.

Bertolani R. & Rebecchi L. 1993. A revision of the *Macrobiotus hufelandi* group (Tardigrada, Macrobiotidae), with some observations on the taxonomic characters of eutardigrades. *Zoologica Scripta* 22: 127–152. https://doi.org/10.1111/j.1463-6409.1993.tb00347.x

Bertolani R., Rebecchi L., Giovannini I. & Cesari M. 2011a. DNA barcoding and integrative taxonomy of *Macrobiotus hufelandi* C.A.S. Schultze 1834, the first tardigrade species to be described, and some related species. *Zootaxa* 2997: 19–36.

Bertolani R., Biserov V., Rebecchi L. & Cesari M. 2011b. Taxonomy and biogeography of tardigrades using an integrated approach: new results on species of the *Macrobiotus hufelandi* group. *Invertebrate Zoology* 8 (1): 23–36.

Bertolani R., Guidetti R., Marchioro T., Altiero T., Rebecchi L. & Cesari M. 2014. Phylogeny of Eutardigrada: New molecular data and their morphological support lead to the identification of new evolutionary lineages. *Molecular Phylogenetics and Evolution* 76: 110–126. https://doi.org/10.1016/j.ympev.2014.03.006

Binda M.G. & Pilato G. 1984. *Macrobiotus sapiens*, nuova specie di Eutardigrado di Sicilia. *Animalia* 11: 85–90.

Binda M.G. & Pilato G. 2001. *Macrobiotus savai* and *Macrobiotus humilis*, two new species of tardigrades from Sri Lanka. *Bolletino delle Sedute dell'Accademia Gioenia di Scienze naturali in Catania* 34: 101–111.

Biserov V.I. 1990a. On the revision of the genus *Macrobiotus*. The subgenus *Macrobiotus* sensu stricto: a new systematic status of the group *hufelandi* (Tardigrada, Macrobiotidae). Communication 1. *Zoologicheskii Zhurnal* 69 (12): 5–17.

Biserov V.I. 1990b. On the revision of the genus *Macrobiotus*. The subgenus *Macrobiotus* s. st. is a new systematic status of the *hufelandi* group (Tardigrada, Macrobiotidae). Communication 2. *Zoologicheskii Zhurnal* 69: 38–50.

Casquet J., Thebaud C. & Gillespie R. 2012. Chelex without boiling, a rapid and easy technique to obtain stable amplifiable DNA from small amounts of ethanol-stored spiders. *Molecular Ecology Resources* 12: 36–41. https://doi.org/10.1111/j.1755-0998.2011.03073.x

Cesari M., Bertolani R., Rebecchi L. & Guidetti R. 2009. DNA barcoding in Tardigrada: the first case study on *Macrobiotus macrocalix* Bertolani & Rebecchi 1993 (Eutardigrada, Macrobiotidae). *Molecular Ecology Resources* 9 (3): 699–706. https://doi.org/10.1111/j.1755-0998.2009.02538.x

Cesari M., Giovanni I., Bertolani R. & Rebecchi L. 2011. An example of problems associated with DNA barcoding in tardigrades: a novel method for obtaining voucher specimens. *Zootaxa* 3104: 42–51.

Dastych 1980. *Niesporczaki (Tardigrada) Tatrzańskiego Parku Narodowego*. Monografie Fauny Polski 9, Polskie Wydawnictwo Naukowe, Kraków.

Degma P. & Guidetti R. 2007. Notes to the current checklist of Tardigrada. *Zootaxa* 1579: 41–53.

Degma P., Bertolani R. & Guidetti R. 2009–2017. Actual checklist of Tardigrada species (2009–2017, 33rd Edition: 15-10-2017). Available from http://www.tardigrada.modena.unimo.it/miscellanea/Actual%20checklist%20of%20Tardigrada.pdf [accessed 23 Dec. 2017].

Folmer O., Black M., Hoeh W., Lutz R. & Vrijenhoek R. 1994. DNA primers for amplification of mitochondrial cytochrome c oxidase subunit I from diverse metazoan invertebrates. *Molecular Marine Biology and Biotechnology* 3: 294–299.

Fontoura P., Pilato G. & Lisi O. 2008. New records of eutardigrades (Tardigrada) from Faial and Pico Islands, the Azores, with the description of two new species. *Zootaxa* 1778: 37–47.

Gąsiorek P., Stec D., Morek W. & Michalczyk Ł. 2018. An integrative redescription of *Hypsibius dujardini* (Doyère, 1840), the nominal taxon for Hypsibioidea (Tardigrada: Eutardigrada). *Zootaxa* 4415 (1): 45-75. https://doi.org/10.11646/zootaxa.4415.1.2

Giribet G., Carranza S., Baguña J., Riutort M. & Ribera C. 1996. First molecular evidence for the existence of a Tardigrada + Arthropoda clade. *Molecular Biology and Evolution* 13: 76–84. https://doi.org/10.1093/oxfordjournals.molbev.a025573

Grigarick A.A., Schuster R.O. & Torftner E.C. 1973. Descriptive morphology of eggs of some species in the *Macrobiotus hufelandi* group (Tardigrada: Macrobiotidae). *Pan–Pacific Entomologist* 49: 258–263.

Guidetti R. & Bertolani R. 2005. Tardigrade taxonomy: an updated check list of the taxa and a list of characters for their identification. *Zootaxa* 845: 1–46. https://doi.org/10.11646/zootaxa.845.1.1

Guidetti R., Gandolfi A., Rossi V. & Bertolani R. 2005. Phylogenetic analysis of Macrobiotidae (Eutardigrada, Parachela): a combined morphological and molecular approach. *Zoologica Scripta* 34: 235–244. https://doi.org/10.1111/j.1463-6409.2005.00193.x

Guidetti R., Schill R.O., Bertolani R., Dandekar T. & Wolf M. 2009. New molecular data for tardigrade phylogeny, with the erection of *Paramacrobiotus* gen. nov. *Journal of Zoological Systematics and Evolutionary Research* 47 (4): 315–321. https://doi.org/10.1111/j.1439-0469.2009.00526.x

Guidetti R., Peluffo J.R., Rocha A.M., Cesari M. & Moly de Peluffo M.C. 2013. The morphological and molecular analyses of a new South American urban tardigrade offer new insights on the biological meaning of the *Macrobiotus hufelandi* group of species (Tardigrada: Macrobiotidae). *Journal of Natural History* 47 (37–38): 2409–2426. https://doi.org/10.1080/00222933.2013.800610

Guil N. & Giribet G. 2012. A comprehensive molecular phylogeny of tardigrades – adding genes and taxa to a poorly resolved phylum-level phylogeny. *Cladistics* 28 (1): 21–49. https://doi.org/10.1111/j.1096-0031.2011.00364.x

Guil N. & Guidetti R. 2005. A new species of Tardigrada (Eutardigrada: Macrobiotidae) from Iberian Peninsula and Canary Islands (Spain). *Zootaxa* 889: 1–11. https://doi.org/10.11646/zootaxa.889.1.1

Hall T.A. 1999. BioEdit: a user-friendly biological sequence alignment editor and analysis program for Windows 95/98/NT. *Nucleic Acids Symposium Series* 41: 95–98.

Heinis F. 1908. Beitrag zur Kenntnis der Moosfauna der Kanarischen Inseln. *Zoologischer Anzeiger* 33: 711–720.

Horning Jr. D.S., Schuster R.O. & Grigarick A.A. 1978. Tardigrada of New Zealand. *New Zealand Journal of Zoology* 5: 185–280. https://doi.org/10.1080/03014223.1978.10428316

Kaczmarek Ł. & Michalczyk Ł. 2017a. A description of *Macrobiotus horningi* sp. nov. and redescriptions of *M. maculatus* comb. nov. Iharos, 1973 and *M. rawsoni* Horning *et al.*, 1978 (Tardigrada: Eutardigrada: Macrobiotidae: *hufelandi* group). *Zootaxa* 4363: 79–100. https://doi.org/10.11646/zootaxa.4363.1.3

Kaczmarek Ł. & Michalczyk Ł. 2017b. The *Macrobiotus hufelandi* group (Tardigrada) revisited. *Zootaxa* 4363: 101–123. https://doi.org/10.11646/zootaxa.4363.1.4

Kaczmarek Ł., Cytan J., Zawierucha K., Diduszko D. & Michalczyk Ł. 2014. Tardigrades from Peru (South America), with descriptions of three new species of Parachela. *Zootaxa* 3790 (2): 357–379. https://doi.org/10.11646/zootaxa.3790.2.5

Katoh K. & Toh H. 2008. Recent developments in the MAFFT multiple sequence alignment program. *Briefings in Bioinformatics* 9: 286–298. https://doi.org/10.1093/bib/bbn013

Katoh K., Misawa K., Kuma K. & Mitaya T. 2002. MAFFT: a novel method for rapid multiple sequence alignment based on fast Fourier transform. *Nucleic Acids Research* 30: 3059–66. https://doi.org/10.1093/nar/gkf436

Kumar S., Stecher G. & Taura K. 2016. MEGA7: Molecular Evolutionary Genetics Analysis version 7.0 for bigger datasets. *Molecular Biology and Evolution* 33: 1870–1874. https://doi.org/10.1093/molbev/msw054

Lanfear R., Frandsen P.B., Wright A.M., Senfeld T. & Calcott B. 2016. PartitionFinder 2: new methods for selecting partitioned models of evolution for molecular and morphological phylogenetic analyses. *Molecular Biology and Evolution* 34: 772–773. https://doi.org/10.1093/molbev/msw260

Mapalo M., Stec D., Mirano–Bascos D.M. & Michalczyk Ł. 2016. *Mesobiotus philippinicus* sp. nov., the first limnoterrestrial tardigrade from the Philippines. *Zootaxa* 4126 (3): 411–426. https://doi.org/10.11646/zootaxa.4126.3.6

Mapalo M., Stec D., Mirano–Bascos D.M. & Michalczyk Ł. 2017. An integrative description of a limnoterrestrial tardigrade from the Philippines, *Mesobiotus insanis*, new species (Eutardigrada: Macrobiotidae: *harmsworthi* group). *Raffles Bulletin of Zoology* 65: 440–454.

Marcus E. 1936. Tardigrada. *Das Tierreich* 66: 1–340.

Marley N.J., McInnes S.J. & Sands C.J. 2011. Phylum Tardigrada: A re-evaluation of the Parachela. *Zootaxa* 2819: 51–64.

Maucci W. 1979. Osservazioni sul valore tassonomico di *Macrobiotus recens* Cuénot, 1932 (Tardigrada, Macrobiotidae). *NATURA–Società italiana di Scienze naturale, Museo civico di Storia naturale e Acquatario civico, Milano* 70: 258–264.

Michalczyk Ł. & Kaczmarek Ł. 2003. A description of the new tardigrade *Macrobiotus reinhardti* (Eutardigrada, Macrobiotidae, *harmsworthi* group) with some remarks on the oral cavity armature within the genus *Macrobiotus* Schultze. *Zootaxa* 331: 1–24.

Michalczyk Ł. & Kaczmarek Ł. 2013. The Tardigrada Register: a comprehensive online data repository for tardigrade taxonomy. *Journal of Limnology* 72 (S1): 175–181. https://doi.org/10.4081/jlimnol.2013.s1.e22

Michalczyk Ł., Wełnicz W., Frohme M. & Kaczmarek Ł. 2012. Redescriptions of three *Milnesium* Doyère, 1840 taxa (Tardigrada: Eutardigrada: Milnesiidae), including the nominal species for the genus. *Zootaxa* 3154: 1–20.

Mironov S.V., Dabert J. & Dabert M. 2012. A new feather mite species of the genus *Proctophyllodes* Robin, 1877 (Astigmata: Proctophyllodidae) from the long-tailed tit *Aegithalos caudatus* (Passeriformes: Aegithalidae): morphological description with DNA barcode data. *Zootaxa* 3253: 54–61.

Morek W., Gąsiorek P., Stec D., Bladgen B. & Michalczyk Ł. 2016a. Experimental taxonomy exposes ontogenetic variability and elucidates the taxonomic value of claw configuration in *Milnesium* Doyère, 1840 (Tardigrada: Eutardigrada: Apochela). *Contributions to Zoology* 85 (2): 173–200.

Morek W., Stec D., Gąsiorek P., Schill R.O., Kaczmarek Ł. & Michalczyk Ł. 2016b. An experimental test of eutardigrade preparation methods for light microscopy. *Zoological Journal of the Linnean Society* 178 (4): 785–793. https://doi.org/10.1111/zoj.12457

Nelson D.R., Guidetti R. & Rebecchi L. 2015. Phylum Tardigrada. *In*: Thorp J.H. & Rogers D.C. (eds) *Ecology and General Biology. Vol. 1: Thorp and Covich's Freshwater Invertebrates (4th edition)*: 347–380 (chapter 17). https://doi.org/10.1016/B978-0-12-385026-3.00017-6

Nowak B. & Stec D. 2018. An integrative description of *Macrobiotus hannae* sp. nov. (Tardigrada: Eutardigrada: Macrobiotidae: *hufelandi* group) from Poland. *Turkish Journal of Zoology* 42: 269–286. https://doi.org/10.3906/zoo-1712-31

Pilato G. 1981. Analisi di nuovi caratteri nello studio degli Eutardigradi. *Animalia* 8: 51–57.

Pilato G. & Bertolani R. 2004. *Macrobiotus dariae* sp. n., a new species of eutardigrade (Eutardigrada, Macrobiotidae) from Cyprus. *Zootaxa* 638: 1–7. https://doi.org/10.11646/zootaxa.638.1.1

Rahm G. 1937. Tardigraden vom Yan-Chia-Ping-Tal (Nordchina). *Zoologischer Anzeiger* 119: 105–111.

Ramazzotti G. 1945. I. Tardigradi d'Italia. *Memorie dell'Istituto italiano di Idrobiologia* 2: 31–166.

Ramazzotti G. 1962. II. Phylum Tardigrada. *Memorie dell'Istituto italiano di Idrobiologia* 16: 1–595.

Ramazzotti G. 1972. Il Phylum Tardigrada (seconda edizione aggiornata). *Memorie dell'Istituto italiano di Idrobiologia* 28: 1–732.

Rambaut A., Drummond A.J., Xie D., Baele G. & Suchard M.A. 2018. Posterior summarisation in Bayesian phylogenetics using Tracer 1.7. *Systematic Biology* syy032. https://doi.org/10.1093/sysbio/syy032

Ronquist F. & Huelsenbeck J.P. 2003. MrBayes 3: Bayesian phylogenetic inference under mixed models. *Bioinformatics* 19: 1572–1574. https://doi.org/10.1093/bioinformatics/btg180

Roszkowska M., Ostrowska M., Stec D., Janko K. & Kaczmarek Ł. 2017. *Macrobiotus polypiformis* sp. nov., a new tardigrade (Macrobiotidae; *hufelandi* group) from the Ecuadorian Pacific coast, with remarks on the claw abnormalities in eutardigrades. *European Journal of Taxonomy* 327: 1–19. https://doi.org/10.5852/ejt.2017.327

Rudescu L. 1946. *Tardigrada*. Fauna Republicii Populare 4 (7), Academiei Republicii Populare Romini, Bucharest.

Sands C.J., McInnes S.J., Marley N.J., Goodall-Copestake W., Convey P. & Linse K. 2008. Phylum Tardigarda: an "individual" approach. *Cladistics* 24: 1–18. https://doi.org/10.1111/j.1096-0031.2008.00219.x

Schill, R.O. & Steinbruck G. 2007. Identification and differentiation of Heterotardigrada and Eutardigrada species by riboprinting. *Journal of Zoological Systematics and Evolutionary Research* 45 (3): 184–190. https://doi.org/10.1111/j.1439-0469.2007.00409.x

Schill R.O., Forster F., Dandekar T. & Wolf N. 2010. Using compensatory base change analysis of internal transcribed spacer 2 secondary structures to identify three new species in *Paramacrobiotus* (Tardigrada). *Organisms Diversity & Evolution* 10 (4): 287–296. https://doi.org/10.1007/s13127-010-0025-z

Srivathsan A. & Meier R. 2012. On the inappropriate use of Kimura–2–parameter (K2P) divergences in the DNA–barcoding literature. *Cladistics* 28: 190–194. https://doi.org/10.1111/j.1096-0031.2011.00370.x

Stec D. & Kristensen R.M. 2017. An integrative description of *Mesobiotus ethiopicus* sp. nov. (Tardigrada: Eutardigrada: Parachela: Macrobiotidae: *harmsworthi* group) from the Northern Afrotropic region. *Turkish Journal of Zoology* 41: 800–811. https://doi.org/10.3906/zoo-1701-47

Stec D., Smolak R., Kaczmarek Ł. & Michalczyk Ł. 2015. An integrative description of *Macrobiotus paulinae* sp. nov. (Tardigrada: Eutardigrada: Macrobiotidae: *hufelandi* group) from Kenya. *Zootaxa* 4052 (5): 501–526. https://doi.org/10.11646/zootaxa.4052.5.1

Stec D., Morek W., Gąsiorek P., Kaczmarek Ł. & Michalczyk Ł. 2016a. Determinants and taxonomic consequences of extreme egg shell variability in *Ramazzottius subanomalus* (Biserov, 1985) (Tardigrada). *Zootaxa* 4208 (2): 176–188. https://doi.org/10.11646/zootaxa.4208.2.5

Stec D., Gąsiorek P., Morek W., Kosztyła P., Zawierucha K., Michno K., Kaczmarek Ł., Prokop Z.M. & Michalczyk Ł. 2016b. Estimating optimal sample size for tardigrade morphometry. *Zoological Journal of the Linnean Society* 178 (4): 776–784. https://doi.org/10.1111/zoj.12404

Stec D., Zawierucha K. & Michalczyk Ł. 2017a. An integrative description of *Ramazzottius subanomalus* (Biserov, 1985) (Tardigrada) from Poland. *Zootaxa* 4300 (3): 403–420. https://doi.org/10.11646/zootaxa.4300.3.4

Stec D., Morek W., Gąsiorek P., Blagden B. & Michalczyk Ł. 2017b. Description of *Macrobiotus scoticus* sp. nov. (Tardigrada: Macrobiotidae: *hufelandi* group) from Scotland by means of integrative taxonomy. *Annales Zoologici* 67 (2): 181–197. https://doi.org/10.3161/00034541ANZ2017.67.2.001

Stec D., Arakawa K. & Michalczyk Ł. 2018a. An integrative description of *Macrobiotus shonaicus* sp. nov. (Tardigrada: Macrobiotidae) from Japan with notes on its phylogenetic position within the *hufelandi* group. *PLoS One* 13 (2): e0192210. https://doi.org/10.1371/journal.pone.0192210

Stec D., Roszkowska M., Kaczmarek Ł. & Michalczyk Ł. 2018b. *Paramacrobiotus lachowskae*, a new species of Tardigrada from Colombia (Eutardigrada: Parachela: Macrobiotidae). *New Zealand Journal of Zoology* 45 (1): 43–60. https://doi.org/10.1080/03014223.2017.1354896

Stec D., Morek W., Gąsiorek P. & Michalczyk Ł. 2018c. Unmasking hidden species diversity within the *Ramazzottius oberhaeuseri* complex, with an integrative redescription of the nominal species for the family Ramazzottiidae (Tardigrada: Eutardigrada: Parachela). *Systematics and Biodiversity* 16 (4): 357–376. https://doi.org/10.1080/14772000.2018.1424267

Stec D., Kristensen R.M. & Michalczyk Ł. 2018d. Integrative taxonomy identifies *Macrobiotus papei*, a new tardigrade species of the *hufelandi* complex (Eutardigrada: Macrobiotidae) from the Udzungwa Mountains National Park (Tanzania). *Zootaxa* 4446 (2): 273–291. https://doi.org/10.11646/zootaxa.4446.2.7

Vaidya G., Lohman D.J. & Meier R. 2011. SequenceMatrix: concatenation software for the fast assembly of multi-gene datasets with character set and codon information. *Cladistics* 27: 171–180. https://doi.org/10.1111/j.1096-0031.2010.00329.x

Vecchi M., Cesari M., Bertolani R., Jönsson K.I., Rebecchi L. & Guidetti R. 2016. Integrative systematic studies on tardigrades from Antarctica identify new genera and new species within Macrobiotoidea and Echiniscoidea. *Invertebrate Systematics* 30 (4): 303–322. https://doi.org/10.1071/IS15033

Wełnicz W., Grohme M.A., Kaczmarek Ł., Schill R.O. & Frohme M. 2011. ITS-2 and 18S rRNA data from *Macrobiotus polonicus* and *Milnesium tardigradum* (Eutardigrada, Tardigrada). *Journal of Zoological Systematics and Evolutionary Research* 49 (S1): 34–39. https://doi.org/10.1111/j.1439-0469.2010.00595.x

Zawierucha K., Kolicka M. & Kaczmarek Ł. 2016. Re-description of the Arctic tardigrade *Tenuibiotus voronkovi* (Tumanov, 2007) (Eutardigrada; Macrobiotidea), with the first molecular data for the genus. *Zootaxa* 4196 (4): 498–510. https://doi.org/10.11646/zootaxa.4196.4.2

Zeller C. 2010. *Untersuchung der Phylogenie von Tardigraden anhand der Genabschnitte 18S rDNA und Cytochrom c Oxidase Untereinheit 1 (COX I)*. MSc Thesis, *Technische Hochschule Wildau*, Germany.

*Manuscript received: 10 April 2018*
*Manuscript accepted: 25 June 2018*
*Published on: 24 July 2018*
*Topic editor: Rudy Jocqué*
*Desk editor: Kristiaan Hoedemakers*

Printed versions of all papers are also deposited in the libraries of the institutes that are members of the *EJT* consortium: Muséum national d'Histoire naturelle, Paris, France; Botanic Garden Meise, Belgium; Royal Museum for Central Africa, Tervuren, Belgium; Natural History Museum, London, United Kingdom; Royal Belgian Institute of Natural Sciences, Brussels, Belgium; Natural History Museum of Denmark, Copenhagen, Denmark; Naturalis Biodiversity Center, Leiden, the Netherlands; Museo Nacional de Ciencias Naturales-CSIC, Madrid, Spain; Real Jardín Botánico de Madrid CSIC, Spain; Zoological Research Museum Alexander Koenig, Bonn, Germany.